EUROPEAN ORGANIZATION FOR NUCLEAR RESEARCH

CERN LIBRARIES, GENEVA

CM-P00043852

CERN/SPSLC 92-19
SPSLC/M491
30 March 1992

Report to the SPS and LEAR Experiments Committee

CP VIOLATION IN HYPERON DECAYS: THE CASE $\overline{p}p \to \overline{\Lambda}\Lambda \to \overline{p}\pi^+ p\pi^-$

CP–Hyperon Study Group:

N. Hamann, X.–G. He, R. Landua, S. Ohlsson, H. Steger, G. Valencia
CERN, Geneva, Switzerland

H. Fischer
Freiburg University, Freiburg, Fed. Rep. Germany

R. Geyer
IMEP Österreichische Akademie der Wissenschaften, Vienna, Austria

D. Hertzog, B. Kolo
University of Illinois, Urbana-Champaign, USA

J.P. Miller
Boston University, Boston, USA

K. Röhrich
IKP Forschungszentrum Jülich, Jülich, Fed. Rep. Germany

Abstract

An account is given of the experimental status of CP violation and of the phenomenology of hyperon non-leptonic decays. Updated information on the estimate of CP-violating observables in these decays is presented. An experimental programme is outlined, with which to pursue the search for direct CP violation in hyperon–antihyperon decays by means of the reaction $\overline{p}p \to \overline{\Lambda}\Lambda \to \overline{p}\pi^+ p\pi^-$. The experiment as well as analysis methods are described. Alternative approaches employing hyperons are discussed as well.

Contents

List of Figures

List of Tables

1 Introduction

Already near the start-up time of the LEAR physics programme, in early 1983, experimentalists presented first arguments [1] about possibilities for measuring CP-violating observables in the non-leptonic decays following the reaction $\bar{p}p \to \overline{\Lambda}\Lambda$. Since then the subject has received increasing interest, both experimentally and theoretically, which has resulted in a correspondingly large number of publications and conference talks. In view of future possibilities at CERN for physics with medium-energy antiprotons, the Proton Synchrotron and Synchro-cyclotron Experiments Committee at its "Cogne V" meeting in September 1990 recommended [2] that a working group be set up in order to investigate:

- the size of CP-violating effects that are theoretically expected in hyperon and anti-hyperon non-leptonic decays;
- the feasibility of an experimental search for CP violation, in particular in the decays $\overline{\Lambda}\Lambda \to \bar{p}\pi^+ p\pi^-$, to be carried out with a suitable antiproton machine.

What follows should be regarded as a (not necessarily complete) progress report of the working group. At this point, we believe that the $\bar{p}p \to \overline{\Lambda}\Lambda \to \bar{p}\pi^+ p\pi^-$ experiment can and should be done. Presently the world's unique machine at which to perform it is LEAR at CERN.

2 Experimental status of CP violation

The non-invariance of the discrete symmetry CP, and its physical origin, is one of the fundamental questions in particle physics. No system, other than the $K^0 - \overline{K}^0$ system, has exhibited CP violation so far. The non-conservation of CP invariance was discovered in 1964 by Christenson, Cronin, Fitch and Turlay [3], who measured a non-zero branching ratio for the decay $K_L \to \pi^+\pi^-$. In this experiment and in most others performed since then [4], the only non-zero measure of CP violation has been the parameter $Re(\epsilon) = (2.258 \pm 0.018) \times 10^{-3}$. Since this parameter defines the mass eigenstates K_S and K_L and the amount of CP impurity in them, the observations have been attributed to a $|\Delta S| = 2$ CP-violating current in the $K^0 \leftrightarrow \overline{K}^0$ transitions.

In on-going experimental programmes at CERN and FNAL the decays of K_S and K_L both into $\pi^0\pi^0$ and $\pi^+\pi^-$ final states have been investigated. Experiment NA31 at the SPS yielded for the first time [5] another non-zero measure of CP violation, its most recent value [6] being: $Re(\epsilon'/\epsilon) = (2.3 \pm 0.7) \times 10^{-3}$. As ϵ' is related to the decay of the pure $CP = -1$ component of K_L, such a 3σ result would constitute experimental evidence for $|\Delta S| = 1$ direct CP violation in the actual two-pion decays of neutral kaons. However, experiment E731 at FNAL, which is similar to NA31 but which measures all four relevant decay modes simultaneously, obtained [7] a different result, the most recent value [8] being: $Re(\epsilon'/\epsilon) = (6.0 \pm 6.9) \times 10^{-4}$.

In the $SU(2) \times U(1)$ Standard Model of electroweak interactions with three quark generations (u,d), (c,s) and (t,b), the quark-mass eigenstates are not the same as the weak eigenstates. The Cabibbo–Kobayashi–Maskawa (CKM) mixing matrix connects the charge $-1/3$ quark-mass eigenstates d, s and b to the weak eigenstates d', s' and b'. Using this convention, the charge $+2/3$ quarks remain unmixed. In addition to rotation angles,

some of the CKM matrix elements naturally contain a phase δ that appears to be the one and only source of CP violation. Both types of CP violation mentioned above can be accommodated [9]:

- the $|\Delta S| = 2$ *indirect CP violation* from mass mixing is created by *box diagrams*, which involve two W-boson exchanges and connect K^0 and $\overline{K}^0$ states to each other;
- the $|\Delta S| = 1$ *direct CP violation* from two-pion decay amplitudes is mainly due to one-loop *penguin diagrams*, which involve exchanges of a single neutral gauge boson (g, γ, Z^0) and connect initial K^0 and final $\pi\pi$ states to each other, and to some extent also due to box diagrams for $K^0 \to \pi\pi$.

While there are *at least three* quark generations required in the Standard Model in order to create CP violation [10, 11], evidence has been forthcoming from LEP and SLC experiments [12] that there are indeed *only three* generations of quarks. However, the mechanism suggested by the Standard Model does not answer the question of the physical origin of CP non-conservation. This will hopefully be answered by present and future experiments searching for new phenomena of CP or T violation [13].

Investigations of K_S and K_L decays into $\pi^0\pi^0$ and $\pi^+\pi^-$ are well established. The new SPS experiment NA48 has recently been approved [14]. It will use combined K_S and K_L beams, the goal being to measure $Re(\epsilon'/\epsilon)$ with an accuracy of 2×10^{-4}. The LEAR experiment PS195 (CPLEAR) has begun an experimental programme [15] using $\overline{p}p$ annihilations at rest, namely $\overline{p}p \to K^+\pi^-\overline{K}^0$ and $\overline{p}p \to K^-\pi^+K^0$, and studying effects of CP violation in two-pion, three-pion, and semi-leptonic decay modes of neutral kaons. In a so-called ϕ-factory [16] operating at $\sqrt{s} = 1.02$ GeV one can measure $Re(\epsilon'/\epsilon)$ by means of the reaction chain $e^+e^- \to \phi \to K_LK_S \to \pi^+\pi^-\pi^0\pi^0$. However, several searches for new signals of CP (or T) violation have been considered in the past years. The most prominent of them are:

- the search for an electric dipole moment of the neutron;
- investigations of certain rare kaon decays, such as $K_L \to \pi^0e^+e^-$, or the observation of longitudinal muon polarization in $K_L \to \mu^+\mu^-$;
- searches for CP violation in the $B^0 - \overline{B}^0$ system, such as the interference between mixing and direct decay diagrams for $(J/\psi + K_S)$ final states;
- investigations of decay asymmetries in hyperon–antihyperon systems, such as $\overline{\Lambda}\Lambda$ or $\overline{\Xi}^-\Xi^-$.

The latter case will be treated in more detail in this report. The idea of testing fundamental symmetries, CP and also CPT, in hyperon non-leptonic decays is not new at all [17, 18, 19, 20, 21]. But only with the advent of intense medium-energy antiproton beams have novel CP-violation experiments based on $\overline{p}p$ annihilation come within reach [22, 23, 24].

As is well known, the exclusive hadronic production of hyperon–antihyperon pairs can provide a particularly clean laboratory. The particles emerge with large polarizations. These are directed transverse to the production plane (owing to parity conservation), and they are equal in magnitude for hyperon and antihyperon (owing to charge-conjugation

invariance). The proton–antiproton initial state is a CP eigenstate, hence the hyperon–antihyperon final state must have the same symmetry [21]. Therefore, hadronic final-state interactions cannot generate a misleading signal. Owing to baryon-number conservation, there is no $\Lambda \leftrightarrow \overline{\Lambda}$ or $\Xi^- \leftrightarrow \overline{\Xi}^-$ mixing, and therefore any observed signal constitutes evidence for $|\Delta S| = 1$ direct CP violation.

3 The parameters ϵ and ϵ' in the Standard Model

The strength of CP violation in the system of neutral kaons is measured by the parameters ϵ and ϵ'. They have been the subject of many theoretical calculations, with the degree of completeness and complexity gradually increasing according to the available experimental information. In the Standard Model with three quark generations the occurrence of CP violation requires that a number of conditions be satisfied [11].

- Quarks with the same charge have to be non-degenerate in mass. This means that it must be $m_u \neq m_c$, $m_c \neq m_t$, $m_t \neq m_u$ and $m_d \neq m_s$, $m_s \neq m_b$, $m_b \neq m_d$.
- All CKM matrix elements must be non-zero and the phase δ must be non-trivial. This means that all three rotation angles have to be different from 0 or $\pi/2$, and that the phase δ must be different from 0 or π.

In the six-quark model the parameters ϵ and ϵ'/ϵ can be expressed [25] as

$$\epsilon = s_{12}\, s_{23}\, s_{13}\, \sin\delta\, T(m_t, s_{ij}, \delta)\,,$$

$$\frac{\epsilon'}{\epsilon} = r\, s_{12}\, s_{23}\, s_{13}\, \sin\delta\, H(m_t)\,.$$

The notation is $s_{ij} = \sin\theta_{ij}$, where the three quark generations are labelled with $\{i, j = 1, 2, 3\}$, and θ_{ij} is the corresponding mixing angle in the CKM matrix. The constant r as well as the functions T and H depend on details of the particular model calculation.

Until a few years ago it was generally assumed that the sixth quark, the top-quark t, was going to be found at a mass below the W-boson mass. Theoretical analyses of ϵ'/ϵ therefore neglected effects pertaining to $m_t > M_W$. With regard to results from $\overline{p}p$ collider experiments at CERN and FNAL the belief is now that the t-quark mass is indeed around 100 GeV at least, but values as high as 250 GeV cannot be excluded. Due to this change towards larger m_t values the theoretical re-examination of the strength of direct CP violation in the Standard Model has become mandatory. Calculations of ϵ'/ϵ for neutral kaons have recently been performed by Buchalla, Buras and Harlander [25] and also by Paschos and Wu [26].

The parameters ϵ and ϵ' are given by

$$\epsilon = \frac{\exp(i\pi/4)}{\sqrt{2}} \left[\frac{ImM_{12}}{\Delta m} + \frac{ImA_0}{ReA_0}\right],$$

$$\epsilon' = -\frac{\exp(i\tilde{\phi})}{\sqrt{2}}\, \frac{ReA_2}{ReA_0} \left[\frac{ImA_0}{ReA_0} - \frac{ImA_2}{ReA_2}\right].$$

Here, M_{12} is the off-diagonal element in the neutral-kaon mass matrix representing all contributions to $K^0 \leftrightarrow \overline{K}^0$ mixing, $\Delta m = 2\,ReM_{12}$ is the $K_L - K_S$ mass difference, A_0

and A_2 are the amplitudes leading to isospin-zero and isospin-two final states in $K^0 \to \pi\pi$, and the relative phase is $\tilde{\phi} = \pi/2 + \delta_2 - \delta_0$ with δ_k denoting the $\pi\pi$ final-state interaction phases for the two possible isospins. Given the experimentally determined values of δ_k we note that the phases of ϵ and ϵ' are nearly equal. From experiments [4] it is also known that $ReA_0 = 3.3 \times 10^{-7}$ GeV, and that $\omega = ReA_2/ReA_0 \approx 1/22$ as expected from the empirical $\Delta I = 1/2$ rule. A non-zero value of ϵ' requires direct CP violation in the $|\Delta S| = 1$ decay amplitudes, whereas a non-zero value of ϵ can arise from $|\Delta S| = 2$ CP-violating effects in the mass matrix or from direct CP violation.

The difficult task is to calculate the decay amplitudes A_0 and A_2, which can be obtained in principle [25, 26] by solving

$$A_k \exp(i\delta_k) = \langle (\pi\pi)_k | \mathcal{H}_{eff}(\Delta S = 1) | K \rangle \, ,$$

where $\mathcal{H}_{eff}(\Delta S = 1)$ is the low-energy effective weak Hamilton operator for the $|\Delta S| = 1$ decays $K^0 \to \pi\pi$. The Hamiltonian contains Wilson coefficient functions $C_i(\mu)$ and 12 four-quark operators $Q_i(\mu)$, the normalization scale μ being of the order of 1 GeV. The basic underlying process in weak interactions of quarks is a quark-flavour transition with four quarks participating, as for example $s+u \to u+d$. Each of the operators Q_i represents a class of diagrams in which the gauge bosons g, γ, Z^0 and W are exchanged in different ways between the participating quarks. The hadronic matrix elements determining the strengths of the various transitions are given by $\langle \pi\pi | Q_i | K \rangle$. Figure 1 shows in its left part examples of a penguin diagram and a box diagram, which both give contributions to direct CP violation in $K^0 \to \pi^+\pi^-$ decays, although of different sizes.

In terms of relevant amplitudes the experimentally accessible ratio ϵ'/ϵ can be written [25] in the form

$$\frac{\epsilon'}{\epsilon} = -\frac{1}{\sqrt{2}\,|\epsilon|} \frac{1}{ReA_0} \frac{ReA_2}{ReA_0} \left[ImA_0 - \frac{ReA_0}{ReA_2} ImA_2 \right] .$$

Here it becomes apparent that ϵ'/ϵ is determined by the phase difference between the transitions to isospin $I = 0$ and $I = 2$ final states. The usual *QCD penguin diagram* involving a gluon exchange generates the amplitude A_0 only. The *electroweak penguin diagrams*, which involve exchanges of Z^0 or γ, jointly contribute to the amplitude A_2. These electroweak contributions can be neglected for $m_t \ll M_W$, but they become increasingly important as m_t grows. With larger m_t values, the decay to $I = 2$ final states can contribute more strongly to ϵ'/ϵ than the decay to $I = 0$ final states, which is due to the enhancement factor $1/\omega = ReA_0/ReA_2 \approx 22$.

Since the phases of transitions to isospin $I = 0$ and $I = 2$ final states turn out to have the same sign, the above formula for ϵ'/ϵ shows a general tendency of cancellation between the A_0 and A_2 parts. Resulting from this, the full calculations performed recently have revealed a rather dramatic dependence on the value of m_t. For most of the m_t range considered ϵ'/ϵ is positive, but it may vanish near $m_t \approx 220$ GeV and become negative at still higher m_t values. This means that in the case of a very heavy top quark the Standard Model behaviour of CP violation can mimic a *superweak theory* [27], in which all CP violation is conceived to originate only from $|\Delta S| = 2$ effects in the mass matrix. However, for the experimentalist this means that it may just be very difficult, if at all possible, to detect direct CP violation in the $K^0 - \overline{K}^0$ system. Somewhat smaller values

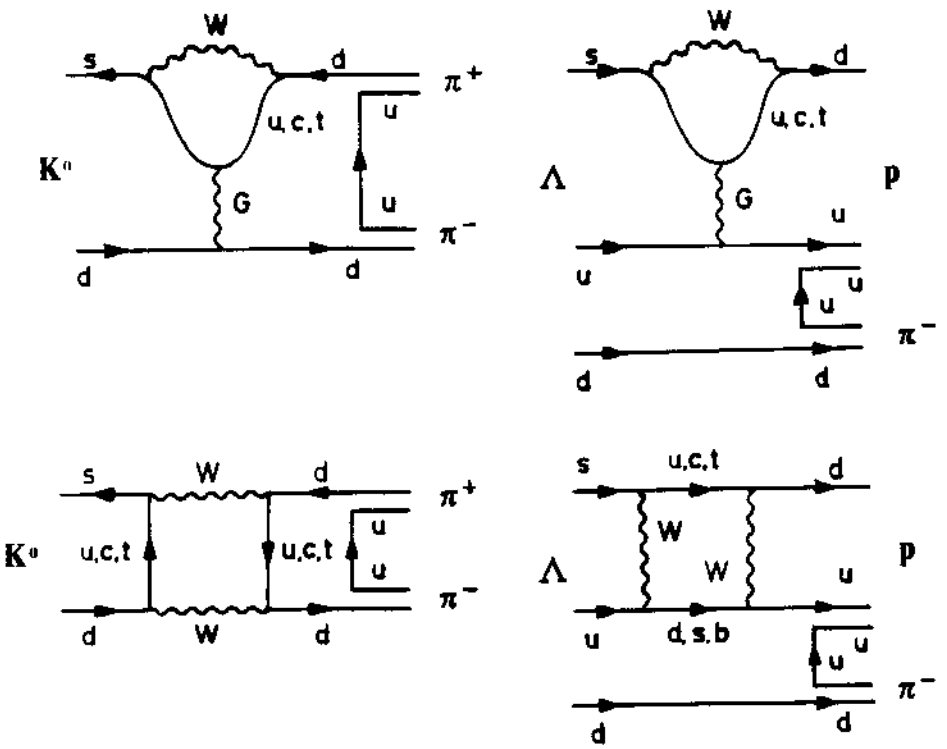

Figure 1: CP-violating penguin and box diagrams. Examples of penguin diagrams (top) and box diagrams (bottom) are shown, which contribute to $|\Delta S| = 1$ direct CP violation in $K^0 \to \pi^+\pi^-$ decays (left) and $\Lambda \to p\pi^-$ decays (right).

$m_t \approx 100$ GeV lead to a range of predictions [25, 26],

$$2 \times 10^{-4} \leq \frac{\epsilon'}{\epsilon} \leq 3 \times 10^{-3} ,$$

where the absolute value is particularly sensitive to the choice of the strange-quark mass m_s. In this region of m_t values the Standard Model is a *milliweak theory*.

In the absence of accurate theoretical predictions, it is important to realize that *any* experiment searching for a signal of direct CP violation in the $K^0 - \overline{K}^0$ system must be designed around *some* number chosen. Therefore, it is *a priori* unknown whether the design sensitivity will be ultimately sufficient to detect CP violation. Clearly, the same is true when considering experiments searching for CP violation in hyperon and antihyperon decays.

4 Phenomenology of hyperon non-leptonic decays

Hyperon non-leptonic decays, such as $\Lambda \to p\pi^-$ ($\overline{\Lambda} \to \overline{p}\pi^+$) or $\Xi^- \to \Lambda\pi^-$ ($\overline{\Xi}^- \to \overline{\Lambda}\pi^+$), proceed by parity-violating weak interactions. Conservation of total angular momentum allows the orbital angular momenta to be $L = 0$ or 1 in the final state. The S-wave case corresponds to the spin vectors of the parent-hyperon and the decay-baryon being equal. Since the final-state parity is $(-1)^{L+1}$, the S-wave decay changes parity from the value

+1 of the parent-hyperon to −1 of the final two-particle state, whereas the P-wave decay conserves parity.

In its most general form the matrix element for the non-leptonic decays of hyperons is given by

$$M = S + P\,\vec{\sigma}\cdot\hat{q}_\pi\,,$$

where S and P are the amplitudes corresponding to $L = 0$ and $L = 1$ decays, respectively, $\vec{\sigma}$ denotes the Pauli spin matrix, and $\hat{q}_\pi$ is the pion momentum unit vector in the hyperon rest frame. Following the notation of Donoghue et al. [28], the partial waves of a given hyperon decay mode can be parameterized in terms of S- and P-wave amplitudes, hadronic pion–baryon final-state interaction phases δ, and weak CP violation phases ϕ, each summed over isospin transitions $|\Delta I| = 1/2$ and $3/2$,

$$S = \sum_{k=1,3} S_k \exp i(\delta_k^S + \phi_k^S)\,,$$

$$P = \sum_{k=1,3} P_k \exp i(\delta_k^P + \phi_k^P)\,.$$

The corresponding antihyperon decay amplitudes are

$$\overline{S} = -\sum_{k=1,3} S_k \exp i(\delta_k^S - \phi_k^S)\,,$$

$$\overline{P} = \sum_{k=1,3} P_k \exp i(\delta_k^P - \phi_k^P)\,.$$

The observables to be formed from the hyperon decay amplitudes are the transition rate

$$\Gamma \propto |S|^2 + |P|^2\,,$$

and the correlation parameters

$$\alpha = \frac{2\,Re(S^*P)}{|S|^2 + |P|^2}\,,$$

$$\beta = \frac{2\,Im(S^*P)}{|S|^2 + |P|^2}\,,$$

$$\gamma = \frac{|S|^2 - |P|^2}{|S|^2 + |P|^2}\,.$$

Since $\alpha^2 + \beta^2 + \gamma^2 = 1$, only two of the three correlation parameters are independent. The parameter α determines the asymmetry of the decay angular distribution, whereas β governs the decay-baryon polarization. One can define an additional parameter ϕ by

$$\beta = \sqrt{1-\alpha^2}\,\sin\phi\,.$$

Correspondingly, the antihyperon decay parameters $\overline{\alpha}$ and $\overline{\beta}$ are expressed in terms of amplitudes $\overline{S}$ and $\overline{P}$.

The violation of CP invariance in the decays can be observed when amplitudes with different phases interfere. For hyperon decays this interference may occur between S- and P-waves or between $|\Delta I| = 1/2$ and $3/2$ transitions. Several experimentally observable

quantities have been considered [21, 28], which, if measured to be non-zero, would signal direct CP violation. These are

$$D = \frac{\Gamma - \overline{\Gamma}}{\Gamma + \overline{\Gamma}} ,$$

$$A = \frac{\Gamma\alpha + \overline{\Gamma}\,\overline{\alpha}}{\Gamma\alpha - \overline{\Gamma}\,\overline{\alpha}} \approx \frac{\alpha + \overline{\alpha}}{\alpha - \overline{\alpha}} ,$$

$$B = \frac{\Gamma\beta + \overline{\Gamma}\,\overline{\beta}}{\Gamma\beta - \overline{\Gamma}\,\overline{\beta}} \approx \frac{\beta + \overline{\beta}}{\beta - \overline{\beta}} ,$$

$$B' = \frac{\Gamma\beta + \overline{\Gamma}\,\overline{\beta}}{\Gamma\alpha - \overline{\Gamma}\,\overline{\alpha}} \approx \frac{\beta + \overline{\beta}}{\alpha - \overline{\alpha}} .$$

Amplitudes with $|\Delta I| = 3/2$ are typically 30 times smaller than those with $|\Delta I| = 1/2$, and the hadronic phases $\sin\delta_k$ are of the order of 0.1. Therefore these quantities need to be considered only in leading order. For the decays $\Lambda \to p\pi^-$ $(\overline{\Lambda} \to \overline{p}\pi^+)$, the size of the signals is then estimated [28] as

$$D \approx \sqrt{2}\,\frac{S_3}{S_1}\,\sin(\delta_3^S - \delta_1^S)\,\sin(\phi_3^S - \phi_1^S) ,$$

$$A \approx \tan(\delta_1^P - \delta_1^S)\,\sin(\phi_1^S - \phi_1^P) ,$$

$$B \approx \cot(\delta_1^P - \delta_1^S)\,\sin(\phi_1^S - \phi_1^P) ,$$

$$B' \approx \sin(\phi_1^S - \phi_1^P) .$$

These estimates are largely model independent. It is important to note that the source of D is an interference between $|\Delta I| = 1/2$ and $3/2$ transitions, whereas the signals A, B and B' are governed by an interference between S- and P-wave amplitudes in the $|\Delta I| = 1/2$ transitions. In principle, B' is the most interesting signal because it is directly determined by the strength $\chi = \sin(\phi_1^S - \phi_1^P)$ of direct CP violation in $|\Delta S| = 1$ hyperon decays. From the above it follows that the relative order of magnitude of the various signals derived from a decay mode is roughly given by

$$0.1\,\mathcal{O}(B) \approx \mathcal{O}(B') \approx 10\,\mathcal{O}(A) \approx 100\,\mathcal{O}(D) .$$

The absolute size of the signals, as predicted in the framework of the Standard Model, is small [28, 29, 30, 31]. In addition, several ingredients used in calculations are of a considerable uncertainty, such as hadronic matrix elements, some elements and the phase δ in the CKM mixing matrix, the quark masses m_s and m_t, and to a lesser extent the value of ϵ'/ϵ. The normalized asymmetries A for the decays $\Lambda \to p\pi^-$ $(\overline{\Lambda} \to \overline{p}\pi^+)$ are a few times 10^{-5} to 10^{-4}. The corresponding values for $\Xi^- \to \Lambda\pi^-$ $(\overline{\Xi}^- \to \overline{\Lambda}\pi^+)$ may be somewhat larger.

A Standard Model calculation of the CP-violation strength χ in hyperon non-leptonic decays has recently been carried out by He, Steger and Valencia [31]. The authors include effects due to a heavy t-quark and make use of recent bounds on the CKM matrix elements. The effective Hamiltonian $\mathcal{H}_{eff}(\Delta S = 1)$ used in the calculation of kaon decays [25] can be used for hyperon decays as well. The basic difference is in the hadronic matrix elements, which are evaluated and compared in several models. Figure 1 shows in its right part examples of a penguin diagram and a box diagram, which give contributions

of different sizes to CP violation in $\Lambda \to p\pi^-$ decays. In particular, for CP violation arising from S- and P-wave interference in hyperon decays there is no overall suppression factor 1/22. Likewise, there is no enhancement of contributions from electroweak penguin diagrams. The ratios A, B and B' are mainly determined by gluon-penguin diagrams referring to $|\Delta I| = 1/2$ transitions. Consequently, the variation of χ as a function of m_t is relatively weak. The authors stress that any numerical result, say $A \approx 0.5 \times 10^{-4}$, has yet incalculable errors associated with it. On the one hand, this is due to the lack of a real framework for computing hadronic matrix elements. On the other hand, experimental knowledge on amplitudes and final-state interaction phases of hyperon decays is rather poor.

The largest CP-testing ratios are B and B', but their measurement requires the determination of the decay-baryon polarization. In case of the decays $\Lambda \to p\pi^-$ and $\overline{\Lambda} \to \bar{p}\pi^+$ this would need a secondary scattering of the outgoing nucleons. However, a direct measurement may be feasible using a *double self-analyzing* decay chain such as $\Xi^- \to \Lambda\pi^- \to p\pi^-\pi^-$ (see Appendix). The ratio D for $\overline{\Lambda}\Lambda$ decays can be measured directly, but this quantity is the smallest one of all. As shown in Section 5 and thereafter, the ratio A for the *single self-analyzing* decays $\Lambda \to p\pi^-$ and $\overline{\Lambda} \to \bar{p}\pi^+$ is relatively easy to be measured, and the accuracy is basically determined by the number of events obtained in the experiment.

5 Initial experimental approaches

5.1 Decay angular distributions

The parity-violating mixture of S- and P-wave decay amplitudes manifests itself in a spatial asymmetry of the decay angular distribution [32, 33]. In the Λ ($\overline{\Lambda}$) rest frame the outgoing proton (antiproton) is emitted preferentially along (opposite to) the parent-spin direction. Owing to this asymmetry the Λ and $\overline{\Lambda}$ non-leptonic decays are called *polarization self-analyzing* [34]. Parity conservation in the hadronic production restricts non-zero components of Λ and $\overline{\Lambda}$ polarizations to be those transverse to the production plane [17], hence $\vec{S}_\Lambda = P_\Lambda \hat{y}$. The production plane is defined by the directions of the incoming beam particle and the outgoing hyperon. However, if these directions are collinear, there is no such plane to be assigned, hence the polarization vanishes [34] at extreme forward or backward centre-of-mass production angles. For a hyperon sample with polarization $P \equiv P_\Lambda$, the normalized angular distribution of the decay protons from $\Lambda \to p\pi^-$ is known to be given by

$$I(\theta_p) = \frac{1}{4\pi}\,(1 + \alpha \vec{S}_\Lambda \cdot \hat{p}_p) = \frac{1}{4\pi}\,(1 + \alpha P\,\cos\theta_p)\,.$$

The angle $\theta_p \equiv \theta_{p_y}$ is measured between the normal to the production plane and the proton direction in the hyperon rest frame, hence $\cos\theta_p = \hat{y} \cdot \hat{p}_p$. The value of the decay-asymmetry parameter, $\alpha = 0.642 \pm 0.013$ for $\Lambda \to p\pi^-$, is known from other experiments [4]. It characterizes the degree of mixing of parities in the decay [33]. We note that the decay angular distribution $I(\theta_p)$ always refers to a given production angle of the hyperons. From the above formula we obtain the expression

$$P = \frac{3}{\alpha}\langle\cos\theta_p\rangle\,,$$

which gives the hyperon polarization in terms of the expectation value of the proton decay angle.

In the limit of CP invariance in hyperon non-leptonic decays, the decay-asymmetry parameters α for $\Lambda \to p\pi^-$ and $\overline{\alpha}$ for $\overline{\Lambda} \to \overline{p}\pi^+$ are expected [17] to be related by $\overline{\alpha} = -\alpha$. The conservation of CP would thus imply $A = 0$, which can be understood from Figure 2 and the following considerations.

1. For a sample of Λ hyperons polarized transverse to the production plane, $\vec{S}_\Lambda = P\,\hat{y}$, one observes that the decay protons are emitted preferentially in the direction of $\vec{S}_\Lambda$, the decay parameter being $\alpha > 0$.

2. The parity transformed of situation 1 is the same sample of Λ particles with the same polarization $\vec{S}_\Lambda$, but with the decay protons being emitted preferentially opposite to the direction of $\vec{S}_\Lambda$. This does not correspond to the observations, because the Λ decay violates parity invariance [32, 33].

3. The charge-conjugation transformed of situation 1 is a sample of $\overline{\Lambda}$ hyperons with the same polarization $\vec{S}_\Lambda$ and with the decay antiprotons being emitted preferentially in the direction of $\vec{S}_\Lambda$. This case is not observed, because the Λ decay violates charge-conjugation invariance [32, 35].

4. The CP-transformed of situation 1 is a sample of $\overline{\Lambda}$ particles with the same polarization $\vec{S}_\Lambda$ and with the decay antiprotons being emitted preferentially opposite to the direction of $\vec{S}_\Lambda$, the decay parameter being $\overline{\alpha} < 0$. This does correspond to the experimental observations. More specifically, however, CP invariance requires that the shape of the decay-proton angular distribution $I(\theta_p)$ be identical to the shape of the decay-antiproton angular distribution $\overline{I}(\theta_{\overline{p}})$. Since the Λ and $\overline{\Lambda}$ polarizations are equal owing to charge-conjugation invariance in the hadronic production process, CP invariance in the weak decays would strictly imply $|\alpha| = |\overline{\alpha}|$, hence $A = 0$.

5.2 Inclusive Λ and $\overline{\Lambda}$ production

All experimental results obtained for hyperons so far are results on the ratio A measured for the decays $\Lambda \to p\pi^-$ and $\overline{\Lambda} \to \overline{p}\pi^+$. We note, however, that they have all been obtained as byproducts of the respective experimental programmes. An experiment dedicated to a high-precision measurement of A has still to be performed.

Experiment R608 at the ISR measured [36] the forward inclusive production of Λ and $\overline{\Lambda}$ hyperons in the reactions $pp \to \Lambda + X$ and $\overline{p}p \to \overline{\Lambda} + X$, respectively, at $\sqrt{s} = 30.8$ GeV. In this experiment, Λ and $\overline{\Lambda}$ particles were thus produced by means of different hadronic reactions. The argument, that the polarization in hyperon production at high energies is a consequence of beam-particle fragmentation, led to the conclusion that Λ produced in pp and $\overline{\Lambda}$ produced in $\overline{p}p$ reactions should have essentially the same polarization. The data sample used for the final result [36] consisted of 17028 Λ and 9553 $\overline{\Lambda}$ particles. The ratio $(\overline{\alpha}\overline{P})/(\alpha P)$ was evaluated, which reduces to $\overline{\alpha}/\alpha$ under the assumption of equal Λ and $\overline{\Lambda}$ polarizations. The weighted average obtained was $\overline{\alpha}/\alpha = -1.04 \pm 0.29$, which can be converted into $A = -0.02 \pm 0.14$.

If one were to aim at much better precision with the method of inclusive production, a major source of systematic errors would come from the fact that the two event samples

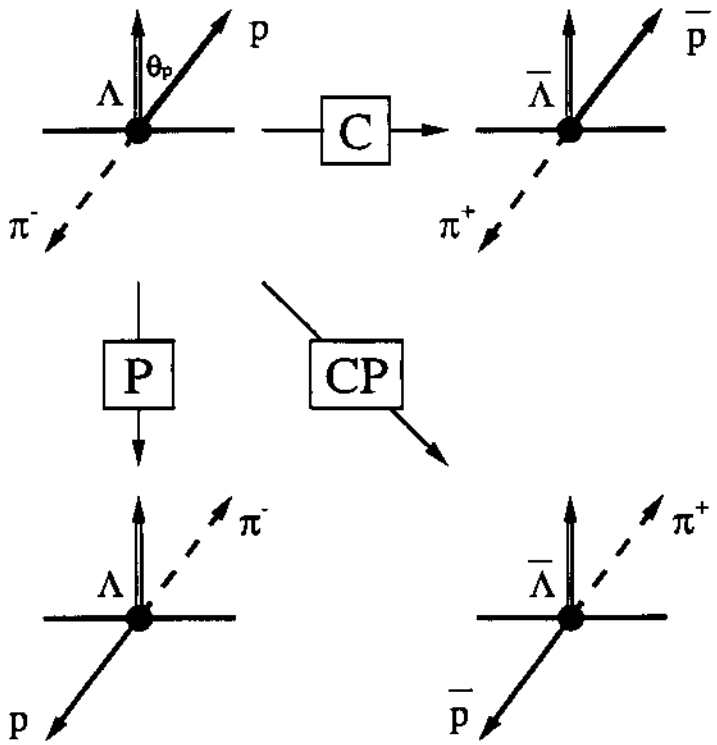

Figure 2: Symmetry transformations for the decay $\Lambda \to p\pi^-$. Schematically shown are the transformations under P (parity), charge conjugation (C), and CP for the decay $\Lambda \to p\pi^-$.

are obtained in separate experimental runs and stem from different hadronic processes. In particular, the assumption that inclusively produced Λ and $\overline{\Lambda}$ particles have equal polarizations is not straightforward and may even not be justified at the per-mille level. In the context of the study presented here, the inclusive production of hyperons and antihyperons is therefore not considered any further.

5.3 Exclusive $\overline{\Lambda}\Lambda$ pair production

The most direct way of comparing Λ and $\overline{\Lambda}$ decay properties is through the exclusive production process $\overline{p}p \to \overline{\Lambda}\Lambda$ as investigated with the PS185 experiment at LEAR. The concept of this experiment is that of a forward-oriented spectrometer for the delayed charged non-leptonic decays of hyperons and antihyperons [37]. One important design feature of the apparatus is its low mass in the way of particles, such that background due to the annihilation of antinucleons is kept at a low level. Another one is the complete solid-angle coverage in the centre-of-mass systems for threshold-type reactions like $\overline{p}p \to \overline{\Lambda}\Lambda$.

The basic components of the PS185 experimental set-up are:

- a target system (CH_2) and a scintillator hodoscope, which together form an on-line trigger for the signature $\overline{p}p \to \textit{neutral} \to \textit{charged}$ of the events sought;
- stacks of multiwire proportional chambers and drift chambers placed in between the target and the hodoscope, which constitute the decay volume for the particles and the tracking volume for their charged decay products;

- a weak-field magnet (0.1 T), which allows hyperons and antihyperons to be distinguished in the off-line analysis.

The principle of the on-line trigger is thus to tag an incoming antiproton, to veto *prompt* charged particles exiting the target, and to detect *delayed* charged particles at some distance (0.5 m) downstream of the target. The off-line reconstruction of the events sought, $\overline{p}p \to \overline{\Lambda}\Lambda \to \overline{p}\pi^+ p\pi^-$, is based mainly on the charged-particle track information provided by the chambers. The experimental set-up includes neither particle identification nor momentum measurement. However, the event reconstruction takes full advantage of various kinematical constraints and of the very distinctive signature of the $\overline{\Lambda}\Lambda$ events.

The polarization analysis yields results on the products αP for $\Lambda \to p\pi^-$ and $\overline{\alpha}\overline{P}$ for $\overline{\Lambda} \to \overline{p}\pi^+$ decays. Charge-conjugation invariance in $\overline{p}p \to \overline{\Lambda}\Lambda$ allows the ratio A to be determined,

$$A = \frac{\alpha + \overline{\alpha}}{\alpha - \overline{\alpha}} = \frac{\alpha P + \overline{\alpha}\overline{P}}{\alpha P - \overline{\alpha}\overline{P}} .$$

A total of 4063 events obtained with the PS185 experiment at 1.546 GeV/c incident antiproton momentum [38] yielded the average value $A = -0.07 \pm 0.09$. The statistics of this measurement combined with another 11362 events obtained at 1.695 GeV/c momentum [37] gave the result $A = -0.024 \pm 0.057$. When taking the previous two data samples together with 44580 events analyzed for 1.642 GeV/c beam momentum [39], one obtains the current best value for A,

$$A = -0.013 \pm 0.029 .$$

The numbers quoted are the averages obtained for the entire centre-of-mass angular range, and the errors are only the statistical ones resulting from the polarization analysis.

6 Problems of polarization analyses

The determination of the ratio A as performed by experiments R608 and PS185 is essentially the analysis of hyperon polarizations from the $\Lambda \to p\pi^-$ and $\overline{\Lambda} \to \overline{p}\pi^+$ decay angular distributions. It is thus equivalent to measurements of the $\cos\theta_p$ and $\cos\theta_{\overline{p}}$ distributions. The values for αP and $\overline{\alpha}\overline{P}$ are obtained independently of each other. In view of its importance in the context discussed in this paper, we will now briefly address some problems related to such a polarization analysis.

Data recorded in the *ideal and perfect detector* would yield a $\Lambda \to p\pi^-$ decay angular distribution which is a straight line in $\cos\theta_p$ with an intercept I_0 and a slope $I_0\,\alpha P$, the hyperon production angle being taken at a fixed value. But a *real and non-perfect detector* produces data that introduce a certain bias in the decay angular distribution. This is due to the fact that only accepted and unambiguously identified events are used in the polarization analysis. However, the acceptance function in the hyperon rest frame is in general not isotropic. As an example we consider small values of $|\cos\theta_p|$, which correspond to decay proton and pion directions in or nearly in the production plane (xz-plane). Because of the boost in the Λ direction ($\hat{z}$), the protons which are emitted nearly opposite to this direction are kinematically correlated with pions emitted at relatively large laboratory angles, $\theta^{lab} \approx 90°$. If such large-angle tracks are not reconstructable due to the detector geometry employed, the acceptance function in the hyperon rest frame has a dip near $|\cos\theta_p| \approx 0$. This will prevent the uncorrected data from falling onto a straight

line in $\cos\theta_p$. Generally speaking, the dependence of the detector acceptance function on decay-nucleon angles with respect to the hyperon direction is more pronounced for smaller hyperon momenta and larger production angles. Clearly, if the polarization is evaluated by means of the straight-line method in $\cos\theta_p$, the necessary acceptance corrections must be determined by means of Monte Carlo simulations. For the PS185 experiment these corrections were estimated to be of the order of 10 %.

In principle such corrections are avoidable because the product αP and its standard deviation $\sigma(\alpha P)$ can be obtained from the data using a *method of weighted sums* [40, 41],

$$\alpha P = \frac{\sum_{i=1}^{N} \cos\theta_p}{\sum_{i=1}^{N} \cos^2\theta_p} ,$$

$$\sigma(\alpha P) = \frac{\sqrt{\sum_{i=1}^{N} \cos^2\theta_p \, (1 - \alpha P \cos\theta_p)^2}}{\sum_{i=1}^{N} \cos^2\theta_p} ,$$

where N is the total number of analyzed events. The error determination takes into account the correlation between the $\cos\theta_p$ and $\cos^2\theta_p$ sums. This method is essentially independent of the bias in the decay angular distributions as discussed above. It requires merely that the acceptance function for the decay nucleons fulfills a symmetry condition in the hyperon rest frame,

$$\eta_{acc}(\theta_p) = \eta_{acc}(180^\circ - \theta_p) .$$

Simulations showed that this symmetry condition is satisfied in the PS185 experiment at the required level of accuracy and that the applied method does not introduce a bias in the polarizations extracted from the real data [37]. For most, but not all, of the polarization analyses the weighted-sums method was therefore used without any acceptance corrections. For practical purposes the determination of the standard deviation of αP can be approximated as

$$\sigma(\alpha P) = \frac{1}{\sqrt{\sum_{i=1}^{N} \cos^2\theta_p}} .$$

We note that under the assumption of an angle-independent acceptance function, which is probably not justified for any *real* detector, the standard deviation of αP would simply reduce to $\sigma(\alpha P) = \sqrt{(3/N)}$.

Whether the polarizations are analyzed by using the straight-line method mentioned first or the weighted-sums method described second, there are in any case many sources of systematic errors that may be encountered in high-statistics experiments such as a CP-violation search.

- *Error in decay angles.* The error in the determination of the quantity $\cos\theta_p$ in PS185 is estimated to be $\Delta(\cos\theta_p) \approx 0.003$ to 0.02, depending on details of the kinematics. This effect contributes to the systematic error of αP at the level of $\Delta(\alpha P) \leq 0.1/\sqrt{N}$, whereas the statistical error is of the order of $\sigma(\alpha P) \approx \sqrt{(3/N)}$.

- *Wrong baryon-number assignment.* A wrong identification of Λ and $\overline{\Lambda}$ vertices has the effect of interchanging the decay-asymmetry parameters $\alpha \leftrightarrow \overline{\alpha} = -\alpha$, the decay angles in the hyperon rest frames $\cos\theta_p \leftrightarrow -\cos\theta_p$, and the centre-of-mass production angles $\cos\theta^* \leftrightarrow -\cos\theta^*$. Therefore, the value of the polarization is still correctly determined, but it is associated with the wrong angular bin. A small

probability (of the order of 1 % in PS185) for assigning wrong baryon numbers has only a small influence on the polarization distribution. In a CP experiment it is not expected to fake an asymmetry signal, however it does have a certain diluting effect on a real asymmetry.

- *Wrong pion–proton identification.* In principle, this is a very dangerous source of error for the determination of the polarization and even more so for a high-statistics CP experiment. If the roles of pion and proton are interchanged for a given $\Lambda \rightarrow p\pi^-$ ($\overline{\Lambda} \rightarrow \overline{p}\pi^+$) vertex, it means reversing the terms *up* and *down* with respect to the reaction plane, hence reversing $P \leftrightarrow -P$. This problem should essentially be eliminated by redundant measurements of the particle momenta in a magnetic field.

- *Acceptance.* It is quite conceivable that the symmetry condition exploited for evaluating polarizations with the weighted-sums method is violated at some level of accuracy in any real and non-perfect detector. A high-precision measurement of the polarization is thus not feasible without a good understanding of the acceptance function. In that sense there is ultimately no advantage of the weighted-sums method over the straight-line method. However, they both mean that αP and $\overline{\alpha}\overline{P}$ are obtained in different and independent procedures, the result of this being that the associated errors may be different and unnecessarily large.

In Section 9 we will outline an alternative method for evaluating the CP-testing ratio A in a high-sensitivity experiment, by means of which the influence of systematic errors can be reduced considerably.

7 Considerations for a high-sensitivity experiment

For the $\overline{\Lambda}\Lambda$ system, the level of sensitivity at which CP violation effects can be conceivably expected is $A \approx 10^{-4}$ or even less. In a dedicated experiment it will be equally important to collect very large event statistics and to control the sources of systematic errors to the required level.

When considering possible experiments with antiproton beams, there are some basic choices to be made [22, 23, 24].

- The two reactions that are particularly well suited are $\overline{p}p \rightarrow \overline{\Lambda}\Lambda$ and possibly $\overline{p}p \rightarrow \overline{\Xi}^-\Xi^-$. The $\overline{\Lambda}\Lambda$ channel allows the asymmetry A to be measured at LEAR, and there is rich information on cross-sections and polarizations available from previous experiments such as PS185. The $\overline{\Xi}^-\Xi^-$ channel is a unique case for the measurement of B and B' at SuperLEAR, but in the absence of experimental data on this reaction the discussion of a high-sensitivity experiment with $\overline{\Xi}^-\Xi^-$ is somewhat academic at present (see Appendix).

- The total centre-of-mass energy chosen determines the production cross-section of the reaction, hence it will influence the statistics of the recorded data. The sensitivity of the experiment is furthermore determined by the shape of the differential cross-section $d\sigma/d\Omega$, as well as by the magnitude and angular distribution of the polarization P. Therefore, the acceptance function has a critical influence on the experimental sensitivity.

- In order to achieve the highest possible luminosity, the experiment should be carried out using a hydrogen cluster-jet or pellet target inserted in the machine. The use of an extracted beam would provide much lower event rates. Colliding $\overline{p}p$ beams have the disadvantage of a rather poor definition of the production vertex.

One limitation of CP-violation experiments discussed here is due to statistics and is merely a question of luminosity and running time. From existing PS185 data the cross-sections and polarizations for $\overline{p}p \to \overline{\Lambda}\Lambda$ are well known. This allows the event statistics necessary for a given precision in A to be estimated rather reliably [42]. For a number of N events the statistical uncertainty on the ratio A is determined as

$$\sigma_A = \frac{1}{\alpha\langle|P|\rangle}\sqrt{\frac{3}{2N}}.$$

Taking $\langle|P|\rangle = 0.27$ as the measured average of the angle-dependent polarization, the precision $\sigma_A \approx 10^{-4}$ corresponds to $N \geq 5 \times 10^9$ events. It is worth noting that the best result on A from PS185 as quoted in Section 5.3, although based on a total of only 60000 events, is entirely consistent with this estimate.

Other limitations are due to experimental asymmetries or systematics, in particular those that affect particles and antiparticles in different ways. The basic experimental problem is to determine the production plane and the directions of the decay nucleons relative to that plane. In a fixed-target experiment on $\overline{p}p \to \overline{\Lambda}\Lambda$ the particles are boosted forward, and the momentum and decay-vertex distributions are in general very different for Λ and $\overline{\Lambda}$ particles. The $\overline{\Lambda}$ angular distribution in the centre-of-mass system is strongly peaked around the direction of the incoming antiproton. Interactions of primary or secondary particles may occur anywhere between production and detection. This includes depolarizing scattering of Λ or $\overline{\Lambda}$ particles before their decay, as well as scattering of decay nucleons and pions before detection. In general, such secondary interactions are different for the decay particles and antiparticles. Care must be taken that the whole experimental arrangement is azimuthally symmetric around the beam axis, the ideal result of this being a *CP-invariant detector*. There should be essentially no difference in the detection efficiencies for particles and antiparticles, and any azimuthal dependence of detection efficiencies should be avoided. The residual polarizations of the beam and the target should be zero. For the magnetic field a solenoidal configuration should be the preferred one, with $\vec{B}$ directed along the beam line.

The high-sensitivity experiment on $\overline{p}p \to \overline{\Lambda}\Lambda$, and that on $\overline{p}p \to \overline{\Xi}^-\Xi^-$ too, requires certain key elements and conditions.

- An antiproton storage ring such as LEAR or SuperLEAR provides a pure and intense beam with a small divergence, good stability, and small momentum spread.

- A hydrogen-cluster jet or, alternatively, a stream of frozen-hydrogen pellets provides a pure proton target, a small interaction region, and a high luminosity.

- The experimental apparatus should comprise sets of fast trigger counters for multiplicity determination and particle identification, low-mass precision chambers for the recording of charged-particle tracks, a solenoidal magnetic field downstream of the interaction region for charge-sign identification and momentum measurement, a selective on-line trigger scheme, and a fast data-acquisition system.

8 The $\overline{p}p \to \overline{\Lambda}\Lambda$ experiment at LEAR-2

8.1 Luminosity at LEAR-2

The CP-violation experiment [42] using $\overline{p}p \to \overline{\Lambda}\Lambda \to \overline{p}\pi^+ p\pi^-$ as proposed here can be performed at LEAR-2. Hereby we mean the LEAR machine, but modified so as to provide a smaller beam pipe and in particular a higher intensity of the antiproton stack. These modifications, one of which consists in raising the injection momentum so as to reduce space-charge effects, have been shown to be achievable with rather *modest and reasonable* cost and effort [43, 44]. The operation of LEAR-2 is assumed to be temporarily dedicated to the CP experiment. Some basic numbers are as follows.

- A hydrogen-cluster jet traverses the antiproton beam perpendicularly. Its initial density is $4 \times 10^{14}\ atoms/cm^3$. Skimmers reduce the size of the jet in the beam direction down to a few mm [45], so that the surface density seen by the antiprotons is $\rho = 10^{14}\ atoms/cm^2$.

- The antiproton stack in the machine consists of $N_0 \geq 2 \times 10^{11}$ particles [43, 44], so that $N_0\,\rho \geq 2 \times 10^{25}\ cm^{-2}$. The beam momentum is 1.65 GeV/c, hence the $\overline{p}p$ invariant mass is just below the $\overline{\Lambda}\Sigma^0 + c.c.$ threshold. At this momentum the revolution frequency is $f = 3.32 \times 10^6\ s^{-1}$.

- The peak luminosity is $L_0 = N_0\,\rho\,f \geq 6.6 \times 10^{31}\ cm^{-2}s^{-1}$. In the course of time the number of particles in the machine decreases, $N(t) = N_0 \exp(-\rho f \sigma_{eff} t)$, where σ_{eff} denotes the total cross-section (hadronic and Coulomb) for absorption and off-acceptance scattering.

- With $\sigma(\overline{p}p \to \overline{\Lambda}\Lambda) \approx 65\ \mu b$ at 1.65 GeV/c and $BR(\Lambda \to p\pi^-) = 0.641$, the production rate of $\overline{p}p \to \overline{\Lambda}\Lambda \to \overline{p}\pi^+ p\pi^-$ events at peak luminosity is $n_0 = L_0\,\sigma\,(BR)^2 \approx 1750\ s^{-1}$.

It is quite clear that not all of the produced events would be recorded by the experiment, the goal being to record the very part that is the most useful for the measurement of A.

8.2 Figure-of-merit and region-of-interest

Data obtained on $\overline{p}p \to \overline{\Lambda}\Lambda$ with PS185 at 1.642 GeV/c beam momentum [39] have been used to probe the sensitivity in various regions of the $\overline{\Lambda}$ production angle $\theta^* \equiv \theta^*_{\overline{\Lambda}}$ in the centre-of-mass system. Figure 3 shows in its top and centre parts the differential cross-section and the polarization, respectively. In the forward region, $d\sigma/d\Omega$ is large and $|P|$ is relatively small. At larger angles $d\sigma/d\Omega$ is flat and relatively small but $|P|$ is large. The statistical uncertainty on the ratio A as quoted in Section 7 is inversely proportional to the product $|P|\sqrt{N}$, hence the polarization has a larger weight than the number of events. In order to make this visible in terms of $\overline{\Lambda}$ production angles, the bottom part of Figure 3 shows the *statistical figure-of-merit*,

$$R = |P| \sqrt{\frac{d\sigma}{d\Omega}}\,,$$

which indicates the region of maximum sensitivity. The measurement of A is obviously most meaningful where R is large. This is the case in the centre-of-mass angular region $-0.75 \leq \cos\theta^* \leq +0.3$. Therefore, particles produced at very small (forward) angles are, although abundant, not particularly useful for the measurement of A.

For an average polarization $\langle|P|\rangle = 0.27$ as measured with PS185 over the full angular range $-1.0 \leq \cos\theta^* \leq +1.0$, the uncertainty $\sigma_A \approx 10^{-4}$ corresponds to $N \geq 5 \times 10^9$ analyzed events. The *region-of-interest*, $-0.75 \leq \cos\theta^* \leq +0.3$, contains more than 25 % of all events and the average polarization is $\langle|P|\rangle = 0.46$ here. For this larger polarization, the same uncertainty $\sigma_A \approx 10^{-4}$ corresponds to $N \geq 1.8 \times 10^9$ analyzed events $\bar{p}p \rightarrow \overline{\Lambda}\Lambda \rightarrow \bar{p}\pi^+ p\pi^-$. Clearly, such a restriction does not mean to reduce the running time of the experiment, but there is a *substantial* reduction of the on-line trigger rate and also a *large* gain in terms of the time and computing power needed to evaluate the data.

8.3 Kinematics

Near 1.65 GeV/c beam momentum the Λ and $\overline{\Lambda}$ particles are emitted at laboratory polar angles $\theta^{lab} \leq 22°$, as shown in the upper left half of Figure 4. Those $\bar{p}p \rightarrow \overline{\Lambda}\Lambda$ events that fall into the region-of-interest in the centre-of-mass system have some distinct features. As can be seen from the upper right half of Figure 4, the laboratory production angles have lower limits too, $\theta^{lab} \geq 10°$ and 16° for the Λ and $\overline{\Lambda}$, respectively. Another feature, visible from the lower half of Figure 4, is that the region-of-interest cut results in less asymmetric, yet not symmetric longitudinal momentum distributions.

For $\overline{\Lambda}\Lambda \rightarrow \bar{p}\pi^+ p\pi^-$ decays, the protons are emitted at laboratory polar angles $\theta^{lab} \geq 6°$, the antiprotons at $\theta^{lab} \geq 10°$, and for both particles the approximate upper limit is $\theta^{lab} \leq 32°$. Almost all decay pions go into the forward hemisphere. The velocities of the nucleons are $\beta \leq 0.75$ and those of the pions are $\beta \leq 0.9$. Therefore, all four decay particles have a time-of-flight (TOF) of at least 8 ns for a 2 m flight path. In fact, the decay pions can have such low momenta that they are not reliably detected. This is a general feature of the reaction under study, and the corresponding event losses are of the order of 10 % even if a rather low minimum momentum of 50 MeV/c is required. However, an experimentally very favourable feature of the events in the region-of-interest is that the distributions of angles and momenta for $\Lambda \rightarrow p\pi^-$ decay products are similar to those of their respective antiparticles from $\overline{\Lambda} \rightarrow \bar{p}\pi^+$ decays. The decay-particle laboratory momentum distributions system are shown in Figure 5.

8.4 Conceptual design of the experiment

The conceptual design of the proposed experiment is shown in Figure 6. It is largely based on today's conventional techniques. The measurement limits itself to those $\overline{\Lambda}\Lambda$ pairs where both particle decays occur in the vacuum of the beam pipe, thereby it eliminates systematic errors due to depolarizing scattering in the beam-pipe material. It is assumed that the beam pipe can be relatively large (diameter $\approx$ 10 cm) upstream of and around the interaction region, but that it must be smaller and have a conical shape (half-angle $\approx 5°$) all the way downstream through the experiment. A thin exit window joins the two sections. The basic detector elements are the following.

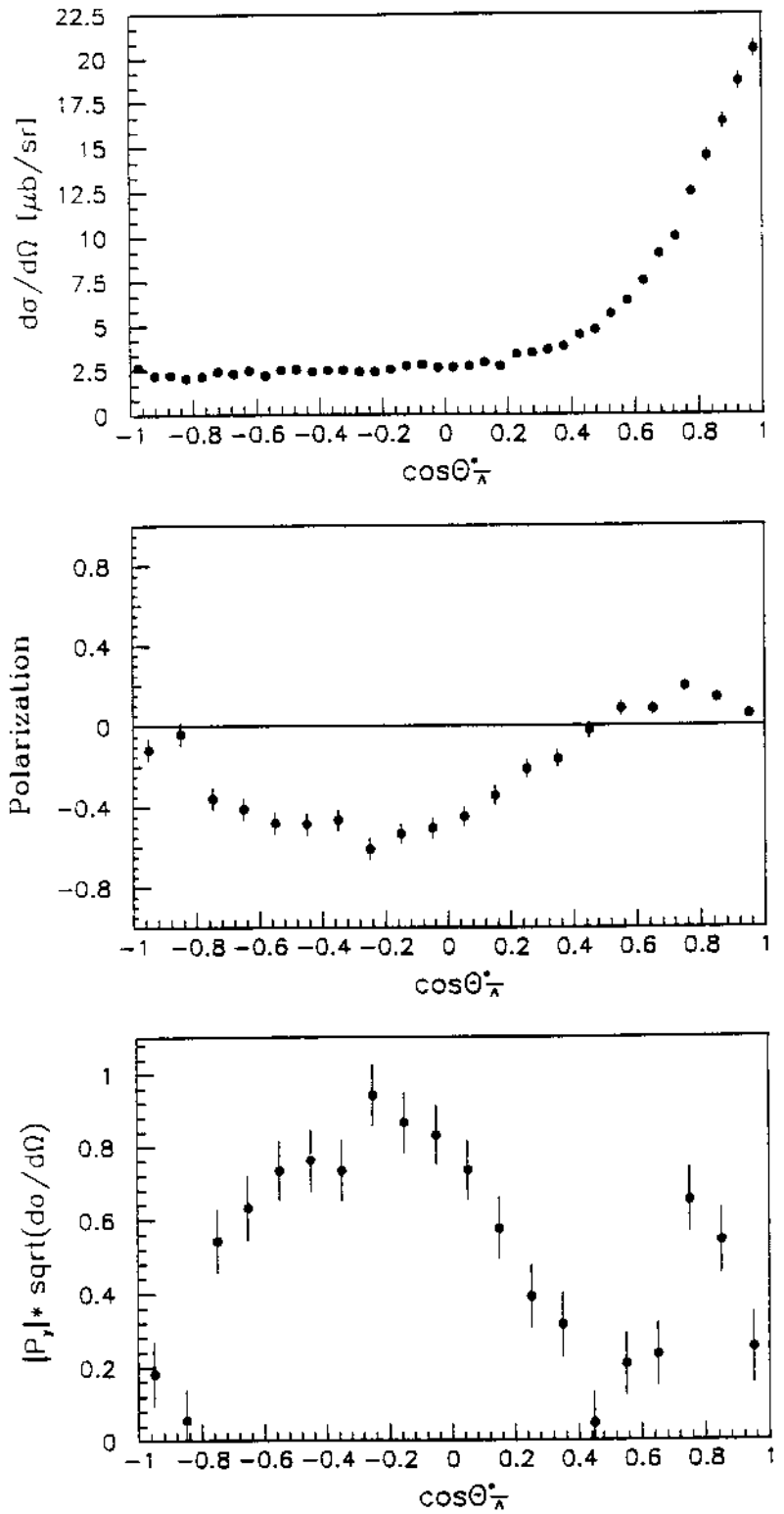

Figure 3: Results on $\bar{p}p \rightarrow \overline{\Lambda}\Lambda$ at 1.642 GeV/c from experiment PS185. Measured data are shown for the differential cross-section $d\sigma/d\Omega$ (top), the hyperon polarization P (centre), and the statistical figure-of-merit $R = |P|\sqrt{(d\sigma/d\Omega)}$ (bottom) as a function of the $\overline{\Lambda}$ production angle in the centre-of-mass system. The data are preliminary and taken from ref. [39].

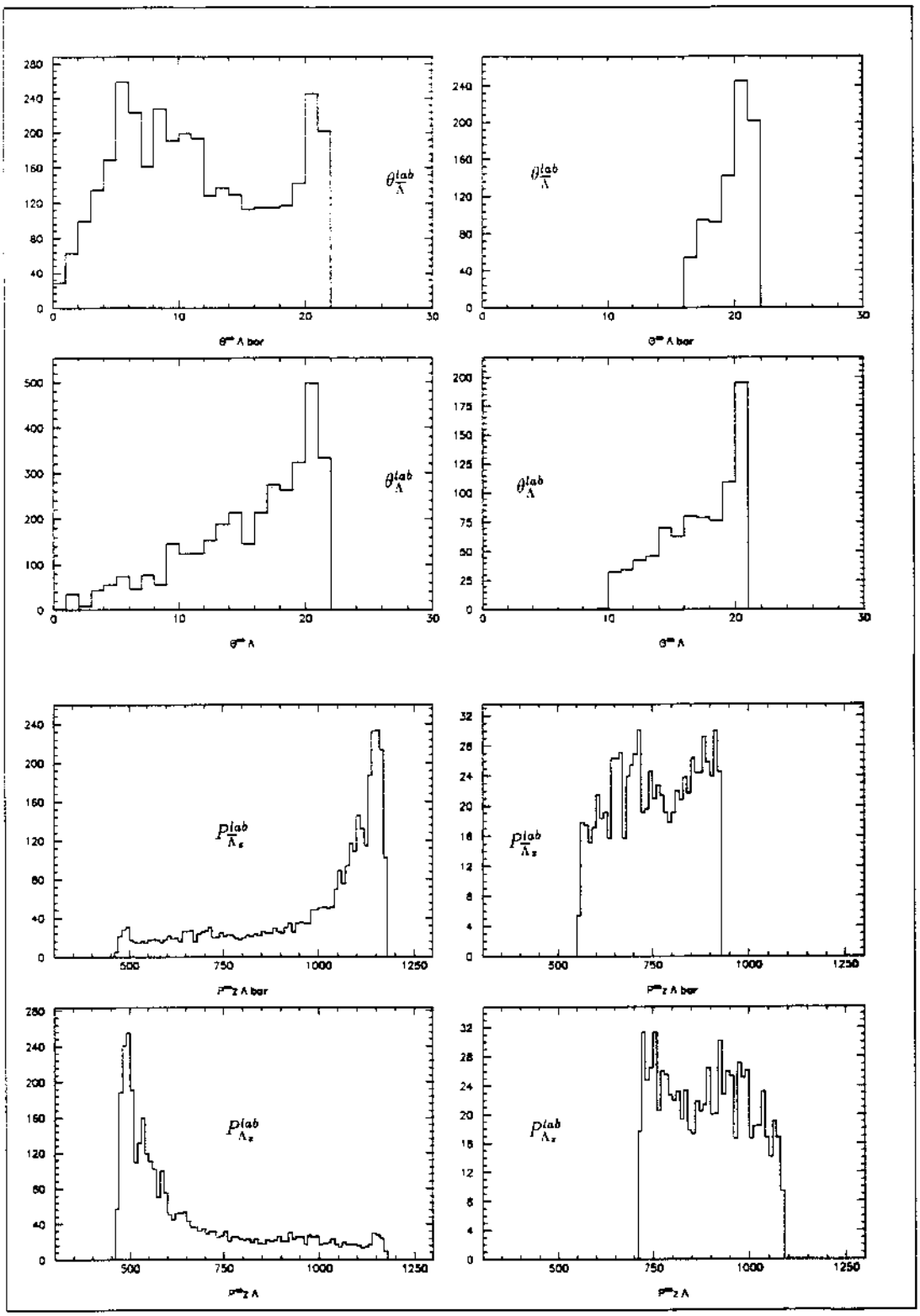

Figure 4: Laboratory angles and momenta for $\overline{p}p \rightarrow \overline{\Lambda}\Lambda$. For data simulated at 1.65 GeV/c incident antiproton momentum shown are, from top to bottom, distributions of the laboratory production angles $\theta_{\overline{\Lambda}}^{lab}$, θ_{Λ}^{lab} (in degrees) and of the laboratory longitudinal momenta $P_{\overline{\Lambda}_z}^{lab}$, $P_{\overline{\Lambda}_z}^{lab}$ (in MeV/c). The plots on the left side include all events, those on the right side only events falling into the region-of-interest.

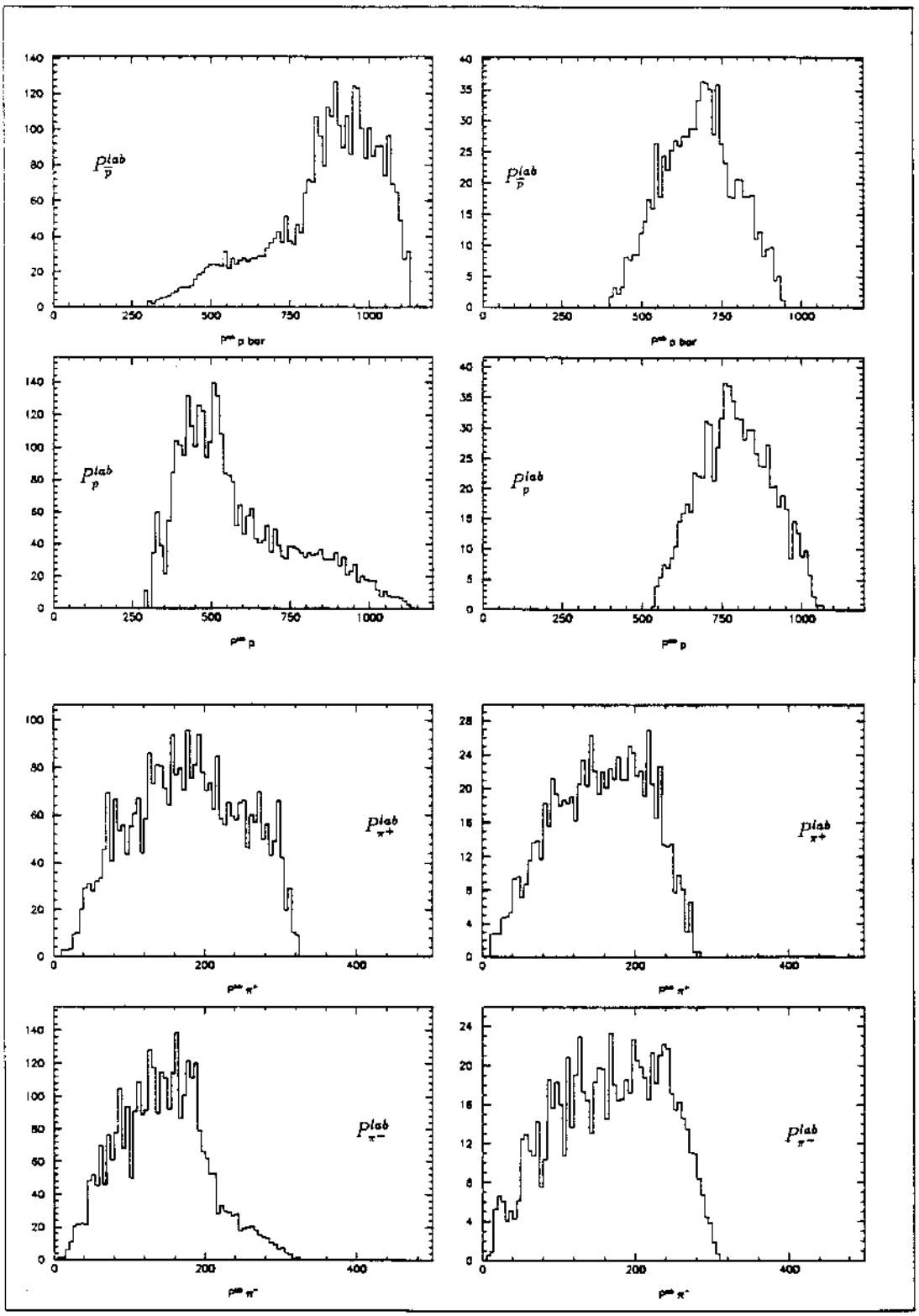

Figure 5: Laboratory momenta for $\overline{\Lambda}\Lambda \rightarrow \overline{p}\pi^+ p\pi^-$ decay products. For $\overline{p}p \rightarrow \overline{\Lambda}\Lambda$ data simulated at 1.65 GeV/c incident antiproton momentum shown are, from top to bottom, distributions of the final-state particle laboratory momenta $P^{lab}_{\overline{p}}$, P^{lab}_{p}, $P^{lab}_{\pi^+}$, $P^{lab}_{\pi^-}$ (in MeV/c). The plots on the left side include all events, those on the right side only events falling into the region-of-interest.

- A counter made of scintillating fibres (SCIFI) is placed immediately behind the exit window of the beam pipe. It provides fast information on charged-particle multiplicities, and it constitutes the nearest space point for tracking. This counter also gives the t_0 reference for time-of-flight and drift-time measurements.

- A 12-layer stack of drift chambers (DC1) is employed for the track recording of charged particles at least up to $\theta^{lab} \leq 65°$.

- Another 12-layer set of drift chambers (DC2) is positioned somewhat downstream so as to provide additional tracking of decay protons and antiprotons at least up to $\theta^{lab} \leq 32°$.

- A scintillator hodoscope (HTOF), segmented in polar and azimuthal directions, is positioned at least 2 m downstream of the SCIFI counter. It measures the time-of-flight of charged particles and provides additional multiplicity information.

- A segmented iron/scintillating fibre calorimeter ($\overline{p}$CAL) identifies the presence of a final-state antiproton.

- Lead/scintillator counters (BAV) placed at backward angles are employed in a mode vetoing photons as well as charged particles.

- A solenoidal magnetic field of strength $B = 0.5$ T begins immediately downstream of the SCIFI counters. It includes the drift chambers as well as the HTOF hodoscope, and the downstream iron return yoke of the magnet incorporates the $\overline{p}$CAL counters. This field provides momentum measurement of charged particles, hence it also serves to distinguish Λ and $\overline{\Lambda}$ vertices.

We note that the experimental set-up does not include a photon detector in the forward hemisphere. On the one hand, radiative decays $\Lambda \to p\pi^-\gamma$ or $\overline{\Lambda} \to \overline{p}\pi^+\gamma$ occur with a branching ratio of only 10^{-3}, the photon energies being relatively low (of the order of 50 MeV and often much less). Simulations showed that these decays do not fake an asymmetry signal at the level of $A \approx 10^{-4}$ discussed here. On the other hand, the rejection of background due to decays $\Sigma^0 \to \Lambda\gamma$ or $\overline{\Sigma^0} \to \overline{\Lambda}\gamma$ is not relevant, because the $\overline{p}p \to \overline{\Lambda}\Lambda$ experiment as conceived here is performed just below the threshold for $\overline{\Lambda}\Sigma^0 + c.c.$ production (1.653 GeV/c incident antiproton momentum).

Key elements foreseen in the first-level on-line trigger include the following conditions:

- four charged particles recorded in the SCIFI counter;

- at least two charged particles within $6° \leq \theta^{lab} \leq 32°$ recorded in the HTOF hodoscope;

- no photon or charged particle at $\theta^{lab} \geq 90°$ recorded in the BAV counter;

- all times-of-flight between the SCIFI counter and the HTOF hodoscope measured to be at least 8 ns for a 2 m flight path;

- an antiproton at $10° \leq \theta^{lab} \leq 32°$ identified by its annihilation signal in the $\overline{p}$CAL counter.

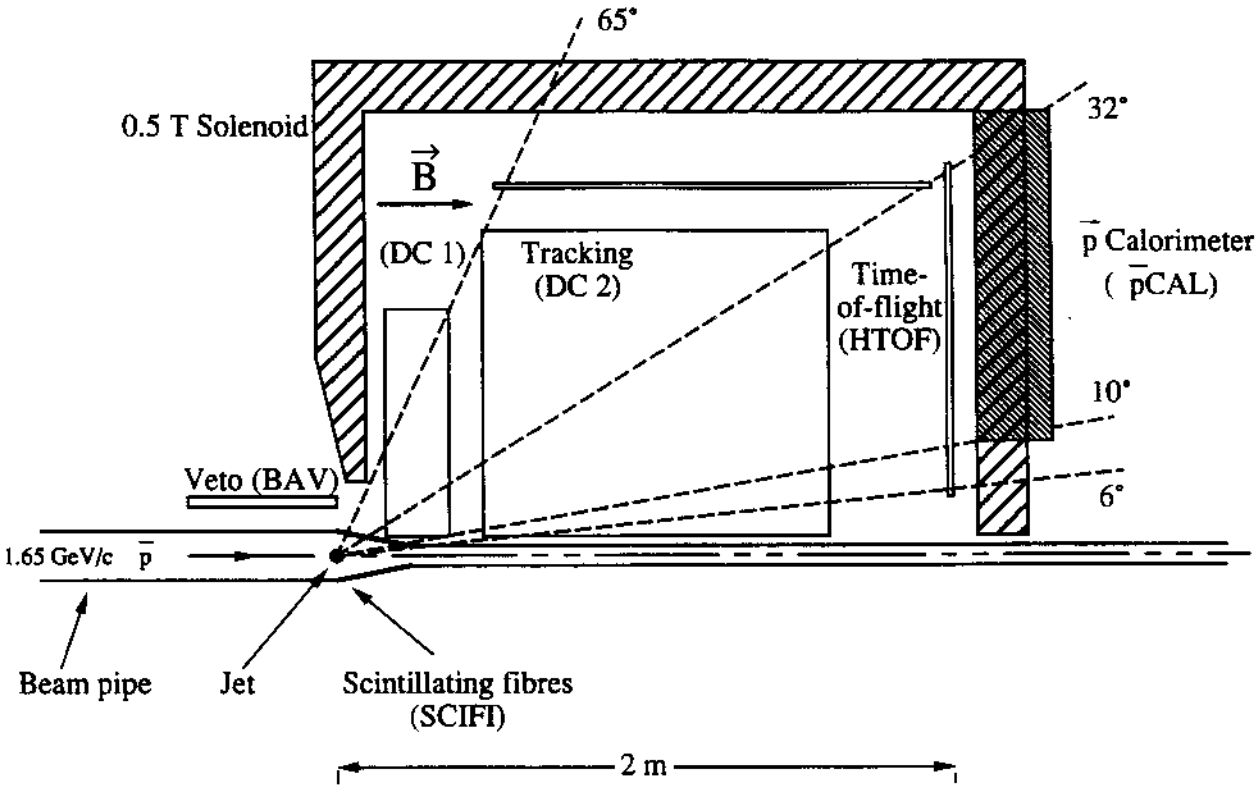

Figure 6: Conceptual design of the $\bar{p}p \rightarrow \overline{\Lambda}\Lambda$ experiment at LEAR-2. The entire detector set-up should be seen to be azimuthally symmetric around the beam axis.

All items of trigger information listed above can be provided at a time scale of a few 100 ns. If deemed necessary, a second-level trigger operating at a scale of a few μs can be employed as well in order to provide further selection and establish four charged-particle tracks.

From the decay-length distributions for Λ and $\overline{\Lambda}$ particles as shown in Figure 7 one may conclude that the SCIFI counter triggering on the presence of four charged particles should be positioned at least 10 cm away from the nominal interaction point. This gives an idea about the geometry of the beam pipe in that region. Time-of-flight distributions for $\overline{\Lambda}\Lambda \rightarrow \bar{p}\pi^+ p\pi^-$ decay products are displayed in Figure 8. One sees that not only lower limits can be imposed on the measured times, but the on-line trigger can employ relatively narrow windows on $(TOF_{max} - TOF_{min})$ in particular for the decay protons and antiprotons.

Based on statistical arguments and on experimental considerations we can estimate the required running time of the proposed experiment.

- At peak luminosity, the production rate of events $\bar{p}p \rightarrow \overline{\Lambda}\Lambda \rightarrow \bar{p}\pi^+ p\pi^-$ falling into the region-of-interest, $-0.75 \leq \cos\theta^* \leq +0.3$, is $\hat{n}_0 = 0.25\, L_0\, \sigma\, (BR)^2 \approx 440\ s^{-1}$.

- The overall efficiency of the experiment is assumed to be 35 %, hence similar to the figure achieved in PS185. This includes the on-line trigger efficiency, the data-acquisition live time, and the off-line reconstruction efficiency.

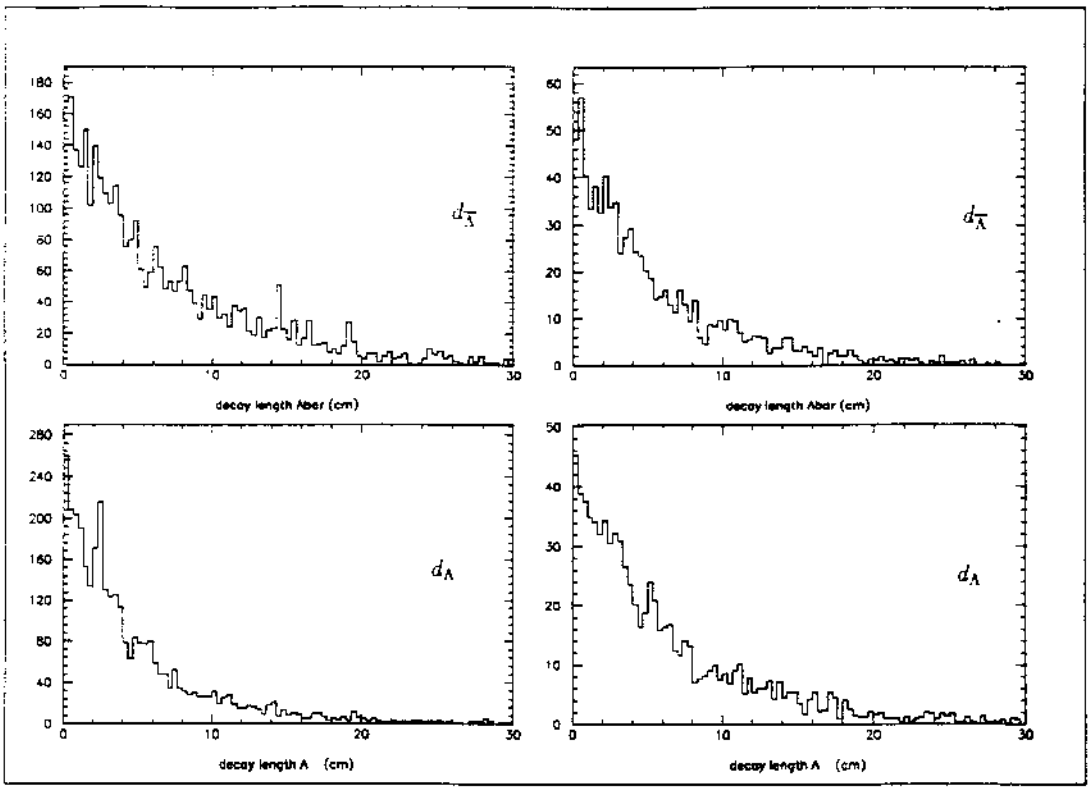

Figure 7: Hyperon decay lengths for $\overline{p}p \to \overline{\Lambda}\Lambda$. For data simulated at 1.65 GeV/c incident antiproton momentum shown are, from top to bottom, distributions of the decay lengths $d_{\overline{\Lambda}}$ and d_{Λ} (in cm). The plots on the left side include all events, those on the right side only events falling into the region-of-interest.

- In order to obtain $N \geq 1.8 \times 10^9$ reconstructable region-of-interest events under the described conditions, for a statistical uncertainty $\sigma_A \approx 10^{-4}$, a running time of 1.2×10^7 s at peak luminosity is required. This is effectively equivalent for the experiment to be *on-beam* at least for one full year.

The required running time is thus *not excessive* but rather typical for a CP-violation experiment.

9 Evaluation of counting asymmetries

9.1 Up–down distributions of final-state particles

The CP-violating ratio A to be measured in $\overline{\Lambda}\Lambda \to \overline{p}\pi^+ p\pi^-$ decays is essentially related to up–down counting asymmetries. These are analyzed in the following, because they provide the best means for extracting CP-testing quantities, and they also allow sources of systematic errors to be understood [46].

Working in the $\overline{p}p$ centre-of-mass system and with $\vec{k}$ denoting the incident beam momentum, a CP-violating triple-product correlation is given [21] by

$$\check{A} = \vec{k} \cdot (\vec{p}_p \times \vec{p}_{\pi^-} - \vec{p}_{\overline{p}} \times \vec{p}_{\pi^+}) = -\vec{k} \times \vec{p}_{\Lambda} \cdot (\vec{p}_p + \vec{p}_{\overline{p}}) \,,$$

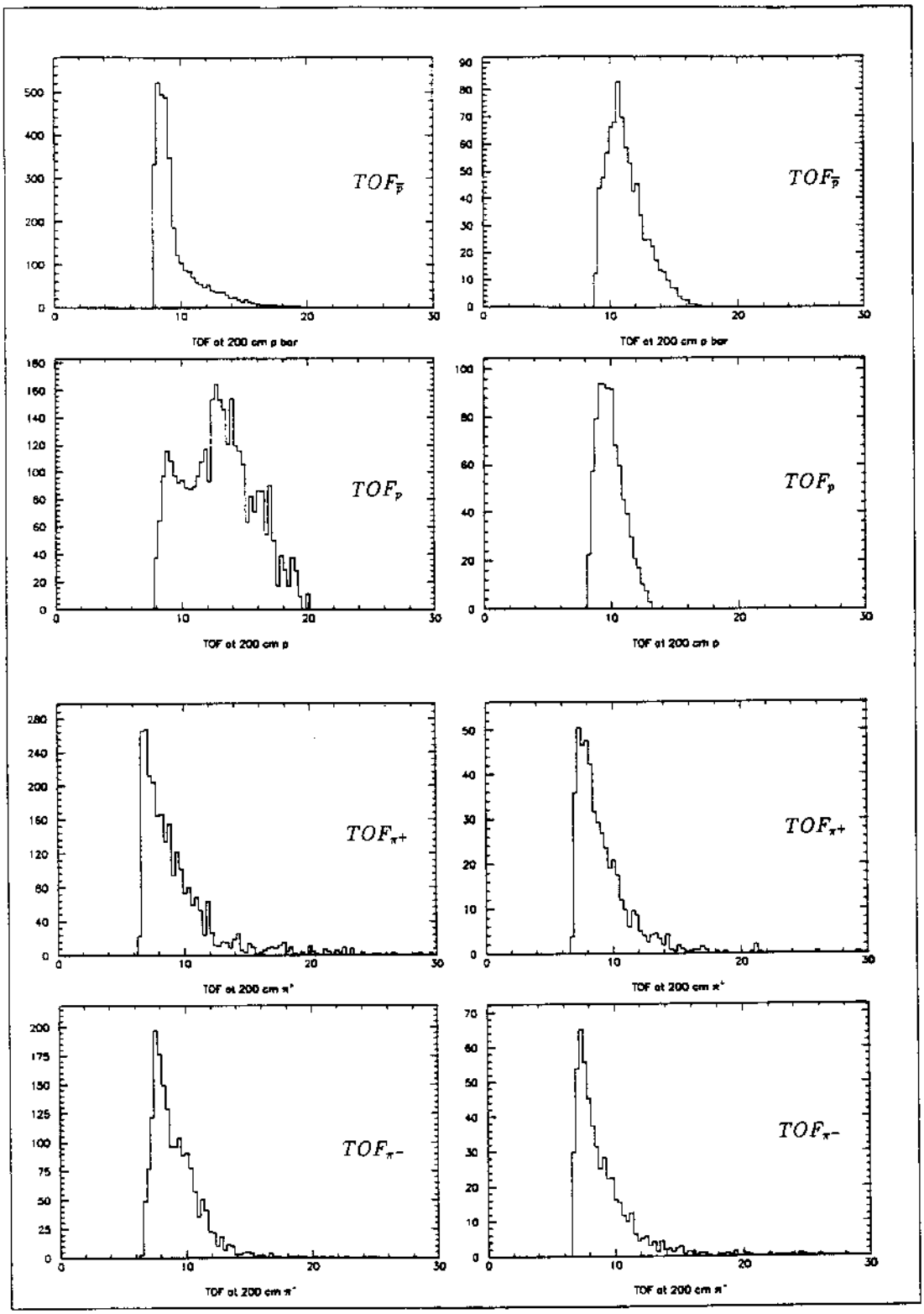

Figure 8: Time-of-flight for $\overline{\Lambda}\Lambda \to \overline{p}\pi^+ p\pi^-$ decay products. For $\overline{p}p \to \overline{\Lambda}\Lambda$ data simulated at 1.65 GeV/c incident antiproton momentum shown are, from top to bottom, distributions of the final-state particle times-of-flight, over a 2 m distance, $TOF_{\overline{p}}$, TOF_p, $TOF_{\pi+}$, $TOF_{\pi-}$ (in ns). The plots on the left side include all events, those on the right side only events falling into the region-of-interest.

where we have used $\vec{p}_\Lambda = \vec{p}_p + \vec{p}_{\pi^-} = -\vec{p}_{\overline{\Lambda}}$. In the first form, $\check{A}$ measures the difference between the correlations of the $\Lambda \to p\pi^-$ and $\overline{\Lambda} \to \overline{p}\pi^+$ decay planes with the beam direction. In the second form, $\hat{A}$ probes the difference between the decay proton and antiproton distributions above and below the reaction plane, the latter being defined by the direction of $\vec{k} \times \vec{p}_\Lambda$. Integrating the above expression over the total number N of events, one obtains the up–down counting asymmetry [21]

$$\tilde{A} = \frac{[N_p(up) + N_{\overline{p}}(up)] - [N_p(down) + N_{\overline{p}}(down)]}{N} ,$$

where up (down) refers to $[\vec{k} \times \vec{p}_\Lambda] \cdot \vec{p}_p > 0\ (< 0)$ in the Λ rest frame. It has been argued [47] that triple-product correlations like the above are sometimes not useful, because their non-zero value may simply arise from final-state interactions. This is not so in the case considered here because the initial $\overline{p}p$ state is a CP eigenstate, so that final-state interactions, if CP conserving, cannot affect the definite CP property.

The numbers of decay protons and antiprotons going up (+) or down (–) with respect to the $\overline{\Lambda}\Lambda$ production plane can be written as

$$N_p(up) = N^{++} + N^{+-} ,$$

$$N_{\overline{p}}(up) = N^{++} + N^{-+} ,$$

$$N_p(down) = N^{-+} + N^{--} ,$$

$$N_{\overline{p}}(down) = N^{+-} + N^{--} ,$$

where the first (second) superscript refers to the proton (antiproton). The total event number being given by $N = N^{++} + N^{+-} + N^{-+} + N^{--}$, we find the relations

$$\frac{N^{++} - N^{--}}{N} = \frac{\alpha + \overline{\alpha}}{4} P \approx A \frac{\alpha}{2} P ,$$

$$\frac{N^{+-} - N^{-+}}{N} = \frac{\alpha - \overline{\alpha}}{4} P \approx \frac{\alpha}{2} P .$$

Apparently, only the "like-sign" events, up–up or down–down, contribute to the CP-testing asymmetry as expressed with A, $\check{A}$ or $\tilde{A}$, whereas "unlike-sign" events, up–down or down–up, cancel trivially. For the counting asymmetry $\tilde{A}$ one obtains

$$\tilde{A} = 2 \frac{N^{++} - N^{--}}{N} = \frac{\alpha + \overline{\alpha}}{2} P \approx A\, \alpha P .$$

9.2 Correlated Λ and $\overline{\Lambda}$ decays

Triple vector products such as those used in $\check{A}$ satisfy $\vec{k} \cdot (\vec{p}_i \times \vec{p}_j) = \vec{p}_i \cdot (\vec{p}_j \times \vec{k}) = \vec{p}_j \cdot (\vec{k} \times \vec{p}_i)$. Therefore, $\check{A}$ is determined by the final-particle momentum components perpendicular to the incident beam momentum $\vec{k}$. This means that $\check{A}$ is invariant under a Lorentz boost in the beam direction, hence it can be expressed in terms of final-particle transverse momenta in the laboratory system [46]. Transverse momentum balance yields

$$-(p_p \cos\vartheta_p + p_{\pi^-} \cos\vartheta_{\pi^-}) = (p_{\overline{p}} \cos\vartheta_{\overline{p}} + p_{\pi^+} \cos\vartheta_{\pi^+}) = q ,$$

$$(p_p \sin\vartheta_p + p_{\pi^-} \sin\vartheta_{\pi^-}) = (p_{\overline{p}} \sin\vartheta_{\overline{p}} + p_{\pi^+} \sin\vartheta_{\pi^+}) = 0 .$$

With $k \equiv |\vec{k}|$, the asymmetry $\check{A}$ becomes

$$\check{A} = k\,[\,p_p\,p_{\pi^-}\sin(\vartheta_{\pi^-} - \vartheta_p) - p_{\overline{p}}\,p_{\pi^+}\sin(\vartheta_{\pi^+} - \vartheta_{\overline{p}})\,] = k\,q^2\,(\sigma_{p\pi^-} - \sigma_{\overline{p}\pi^+})\,,$$

where we have defined and used

$$\sigma_{ij} = \frac{\sin\vartheta_i\,\sin\vartheta_j}{\sin(\vartheta_j - \vartheta_i)} = \frac{1}{\cot\vartheta_i - \cot\vartheta_j}\,.$$

Clearly, the above is valid for all values of k and q. CP violation would thus be indicated by a non-zero value of

$$\check{a} = \sigma_{p\pi^-} - \sigma_{\overline{p}\pi^+}\,,$$

and this can be determined just from angle measurements in the transverse plane.

We assume that $\overline{\Lambda}$ is produced with a transverse momentum $\vec{q}$. In the $\overline{\Lambda}$ rest frame the decay particles $\overline{p}$ and π^+ emerge with momenta $p_{dec} = 101$ MeV/c directed back-to-back. For these decay momenta we consider three orthogonal components each: parallel to the incident beam ($\hat{z}$), normal to the production plane ($\hat{y}$), and transverse to the beam but in the production plane ($\hat{x} = \hat{y} \times \hat{z}$). The boost from the $\overline{\Lambda}$ rest frame has $\gamma\beta = q/m_\Lambda$. It turns out that the ratios of the transverse momentum components along $\hat{x}$ and $\hat{y}$ for $\overline{p}$ and π^+ are just $\cot\vartheta_{\overline{p}}$ and $\cot\vartheta_{\pi^+}$, respectively. The corresponding boost from the Λ rest frame has $\gamma\beta = -q/m_\Lambda$. For the decays $\Lambda \to p\pi^-$ and $\overline{\Lambda} \to \overline{p}\pi^+$ the transformation yields

$$\sigma_{p\pi^-} = -\frac{p_{dec}}{q}\cos\theta_p\,,$$

$$\sigma_{\overline{p}\pi^+} = \frac{p_{dec}}{q}\cos\theta_{\overline{p}}\,.$$

Inserting this in the above expressions for $\check{A}$ and $\check{a}$, we find for the asymmetry [46]

$$\check{A} = k\,q^2\,\check{a} = -k\,q\,p_{dec}(\cos\theta_p + \cos\theta_{\overline{p}})\,.$$

When one considers the decays $\Lambda \to p\pi^-$ and $\overline{\Lambda} \to \overline{p}\pi^+$ simultaneously, the angular distribution of events is given by [21, 37]

$$\frac{d^2N}{d(\cos\theta_p)\,d(\cos\theta_{\overline{p}})} = \frac{1}{16\pi^2}\,[\,1 + \alpha P\cos\theta_p + \overline{\alpha}P\cos\theta_{\overline{p}} + \alpha\overline{\alpha}\sum_{i,j=x,y,z} C_{ij}\,\cos\theta_{p_i}\,\cos\theta_{\overline{p}_j}\,]\,,$$

where C_{ij} denote the $\Lambda - \overline{\Lambda}$ spin-correlation coefficients. The well-known independent Λ and $\overline{\Lambda}$ decay angular distributions, $I(\theta_p) = dN/d(\cos\theta_p)$ and $\overline{I}(\theta_{\overline{p}}) = dN/d(\cos\theta_{\overline{p}})$, respectively, are obtained by integration over the emission angle of the non-observed particle.

The space spanned by $\cos\theta_p$ and $\cos\theta_{\overline{p}}$ has four quadrants which are filled with event samples given by the following numbers:

$$N^{++} = \frac{N}{4}(1 + \frac{\alpha + \overline{\alpha}}{2}\,P + \frac{\alpha\overline{\alpha}}{4}\,C_{yy})\,,$$

$$N^{+-} = \frac{N}{4}(1 + \frac{\alpha - \overline{\alpha}}{2}\,P - \frac{\alpha\overline{\alpha}}{4}\,C_{yy})\,,$$

$$N^{--} = \frac{N}{4}(1 - \frac{\alpha + \overline{\alpha}}{2}\,P + \frac{\alpha\overline{\alpha}}{4}\,C_{yy})\,,$$

$$N^{-+} = \frac{N}{4}\,(1 - \frac{\alpha - \overline{\alpha}}{2}\,P - \frac{\alpha\overline{\alpha}}{4}\,C_{yy})\,,$$

where for reasons of simplicity we have considered only the diagonal spin-correlation coefficient with respect to the normal of the production plane. Obviously a revelation of CP non-invariance would be given if the event distribution in the $(\cos\theta_p, \cos\theta_{\overline{p}})$ plane shows a non-zero expectation value $\langle\cos\theta_p + \cos\theta_{\overline{p}}\rangle$.

In terms of new variables, defined as $u = (\cos\theta_p + \cos\theta_{\overline{p}})/2$ and $v = (\cos\theta_p - \cos\theta_{\overline{p}})/2$, the combined angular distribution of events can be rewritten as

$$\frac{d^2N}{du\,dv} = \frac{1}{8\pi^2}\,[\,1 + (\alpha + \overline{\alpha})P\,u + (\alpha - \overline{\alpha})P\,v + \alpha\overline{\alpha}\,C_{yy}\,(u^2 - v^2)\,]\,,$$

where again only C_{yy} has been included in the spin-correlation term. For a given value of v, the case of which represents the main diagonal or a line parallel to it in the $(\cos\theta_p, \cos\theta_{\overline{p}})$ plane, one finds that

$$\frac{dN}{du}\,|_u - \frac{dN}{du}\,|_{-u} \propto (\alpha + \overline{\alpha})P\,u = 2\,\tilde{A}\,u\,.$$

Apparently, the asymmetry between the two half-planes, $u > 0$ and $u < 0$, is a direct measure of CP violation [46]:

$$\dot{A} = \frac{\int_0^1\int_{-1}^1 \frac{d^2N}{du\,dv}\,dv\,du - \int_0^{-1}\int_{-1}^1 \frac{d^2N}{du\,dv}\,dv\,du}{\int_0^1\int_{-1}^1 \frac{d^2N}{du\,dv}\,dv\,du + \int_0^{-1}\int_{-1}^1 \frac{d^2N}{du\,dv}\,dv\,du}\,.$$

An obvious advantage of measuring the event distribution in the $(\cos\theta_p, \cos\theta_{\overline{p}})$ plane over independent analyses of αP and $\overline{\alpha}\overline{P}$ (see Section 6) is that the new method makes use of *all* events. The described procedure fully exploits the fact that in *all* four quadrants the events have *non-uniform* distributions governed by the polarizations and the spin correlations of Λ and $\overline{\Lambda}$ particles. This can be visualized when projecting the events onto the main diagonal representing the variable u for $v = 0$, and comparing the obtained distribution in the two intervals $-1 \leq u < 0$ and $0 < u \leq 1$. Another advantage of the new method is that the influence of systematic errors is reduced considerably.

We have used PS185 data measured at 1.642 GeV/c incident antiproton momentum for illustrating the counting asymmetries discussed above. Figure 9 shows a two-dimensional event distribution in the $(\cos\theta_p, \cos\theta_{\overline{p}})$ plane for the decays $\overline{\Lambda}\Lambda \to \overline{p}\pi^+ p\pi^-$. The plot contains only those events that fall into the region-of-interest, $-0.75 \leq \cos\theta^* \leq +0.3$. Since $P < 0$ in all of this range, the density of events in Figure 9 decreases monotonically from top-left ($\cos\theta_p < 0$ and $\cos\theta_{\overline{p}} > 0$) to bottom-right ($\cos\theta_p > 0$ and $\cos\theta_{\overline{p}} < 0$).

The intensity distribution of $\overline{\Lambda}\Lambda \to \overline{p}\pi^+ p\pi^-$ decays measured with PS185 is also visible in the projections of Figure 9 as shown in the top and centre parts of Figure 10. The distribution along $\cos\theta_p$ ($\cos\theta_{\overline{p}}$) has slopes $\alpha P < 0$ ($\overline{\alpha}P > 0$). We note that straight lines would not be expected here, because the data in Figures 9 and 10 correspond to a range in $\cos\theta^*$ over which the polarization varies in magnitude. The distribution relevant for the CP-testing ratio $\dot{A}$ is obtained when projecting the events of Figure 9 onto the main diagonal representing the variable u for $v = 0$. The result of this is shown in the bottom part of Figure 10. Comparing the right ($u > 0$) and left ($u < 0$) halves, or equivalently in Figure 9 the two half-planes separated by $u = 0$, we find

$$\dot{A} = \frac{N(u > 0) - N(u < 0)}{N(u > 0) + N(u < 0)} = -0.011 \pm 0.021\,,$$

where only the statistical error is given.

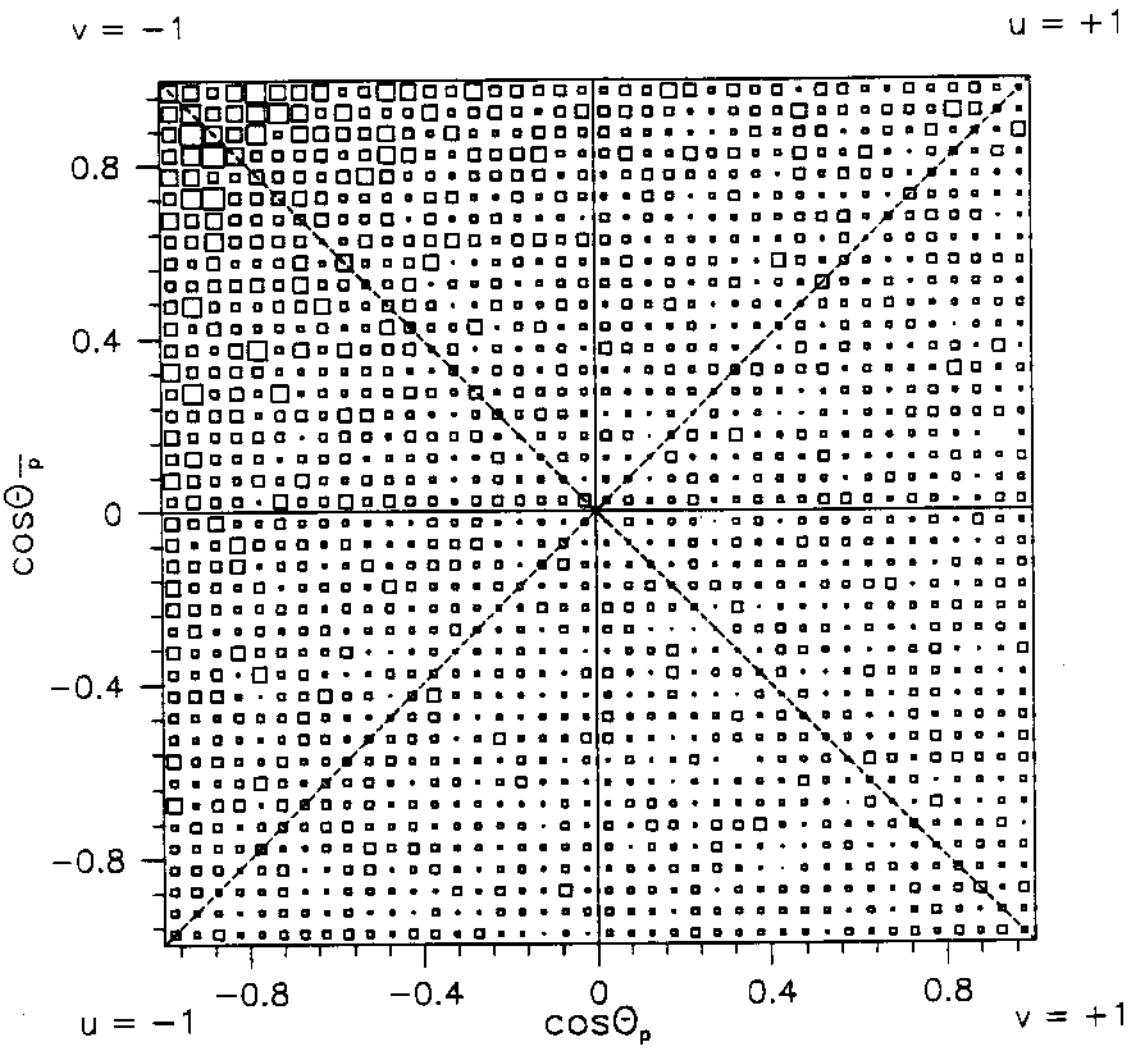

Figure 9: Correlation in $\overline{\Lambda}\Lambda \to \bar{p}\pi^+ p\pi^-$ decays measured with PS185. For data taken at 1.642 GeV/c incident antiproton momentum, the plot shows the $(\cos\theta_p, \cos\theta_{\bar{p}})$ distribution of events falling into the region-of-interest, $-0.75 \leq \cos\theta^* \leq +0.3$. Also indicated are the two diagonals representing the variables u (for $v = 0$) and v (for $u = 0$), respectively.

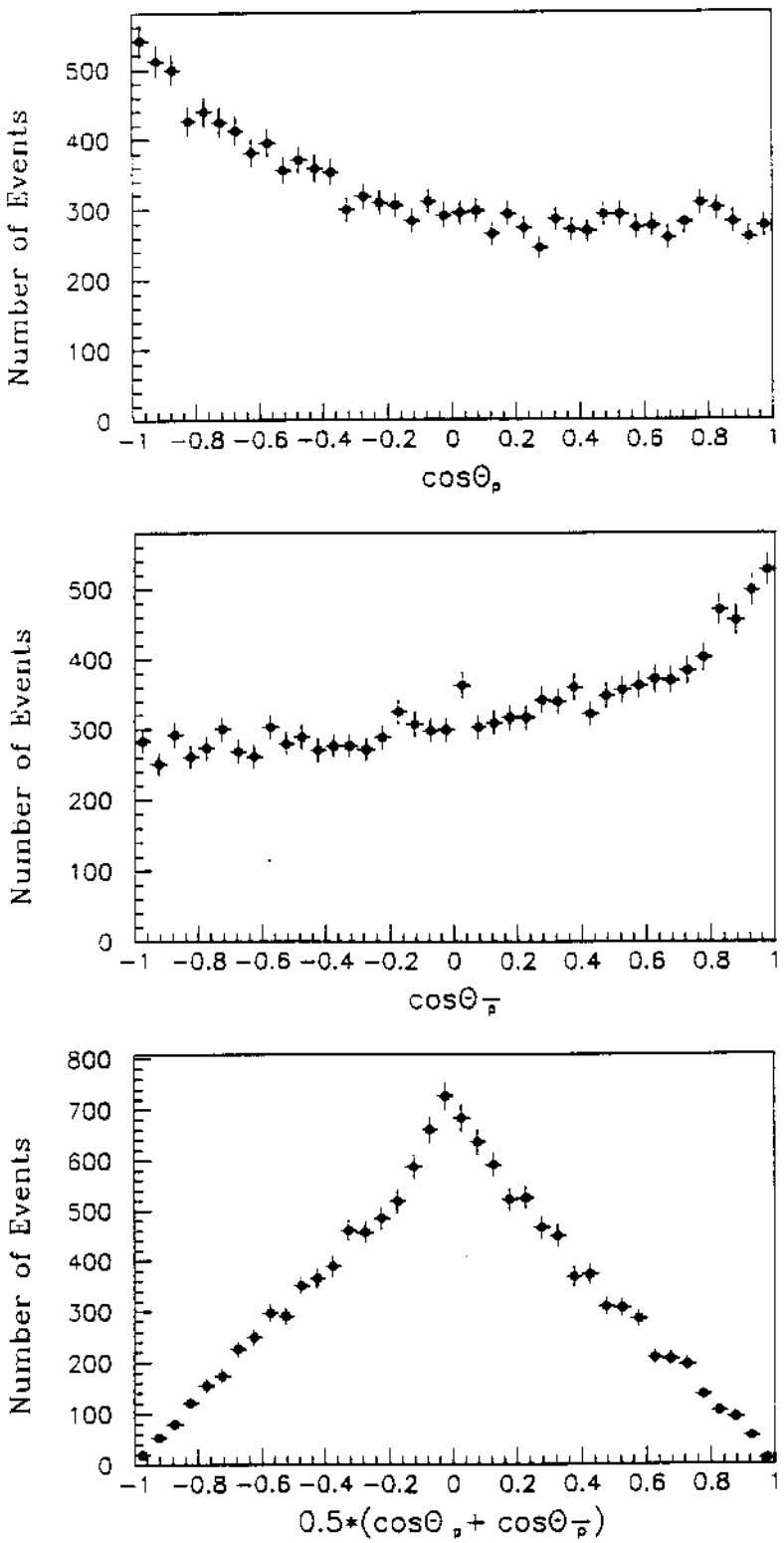

Figure 10: Region-of-interest $\overline{\Lambda}\Lambda \rightarrow \overline{p}\pi^+ p\pi^-$ decay distributions. Based on the 1.642 GeV/c data of PS185 displayed in Figure 9, the projections are shown onto the axes given by $\cos\theta_p$ (top) and $\cos\theta_{\overline{p}}$ (centre), and onto the main diagonal representing $u = (\cos\theta_p + \cos\theta_{\overline{p}})/2$.

10 Systematic errors

It is clear that all possible systematic errors must be thoroughly studied before a high-sensitivity experiment on CP (non-)conservation in the $\overline{\Lambda}\Lambda \rightarrow \bar{p}\pi^+ p\pi^-$ decays can be endorsed. We have begun to explore this important topic and the discussion presented below is meant to illustrate the types of concerns we have uncovered and some of the cures which we recommend. Almost by definition, there are effects which we have not thought of, as the study of systematic errors in any such experiment is a continual process.

It should be emphasized again that the principle of the experiment as proposed here consists in the *exclusive* production of $\overline{\Lambda}\Lambda$ pairs, the non-leptonic charged decay of these particles in the *vacuum*, and the unambiguous identification of *all four* decay products from $\Lambda \rightarrow p\pi^-$ and $\overline{\Lambda} \rightarrow \bar{p}\pi^+$. The essence of the measurement is a sophisticated counting exercise of decay protons and antiprotons (or π^- and π^+) going above or below the production plane. The latter is defined by the vertices of the Λ and $\overline{\Lambda}$ decays and the original interaction location. To the extent that the efficiency for detecting decay nucleons travelling above (up) the production plane is the same as that for decay nucleons going below (down), the measurement should be on firm grounds. But, as we will illustrate below, it is more complicated than that.

10.1 Basic assumptions

We note here a few of the assumptions which permit the extraction of the quantity $A = (\alpha + \overline{\alpha})/(\alpha - \overline{\alpha})$ from the observations. First, we assume that C, P and CP are conserved in the hadronic production process $\bar{p}p \rightarrow \overline{\Lambda}\Lambda$. In fact, this is not tested at the required level for the measurement here, but would represent an even greater problem for the Standard Model than a CP violation in the weak decay process does. Second, we assume that both the beam and the target are unpolarized. Any small residual polarization of the antiproton beam stored in LEAR could preferentially distort the required equality that $P_\Lambda = P_{\overline{\Lambda}}$. We expect that the polarization transfer T is small, the spin of the Λ and $\overline{\Lambda}$ essentially being carried by the produced strange and antistrange quarks. However, in the technical implementation of the antiproton machine it may be necessary to include some mechanism explicitly to depolarize the beam or, alternatively, to rotate the spin of the antiprotons rapidly and randomly as the effect would enter linearly in the product $P_\Lambda T$ in the quantity A. The possibility of selective depolarization of the Λ and the $\overline{\Lambda}$ is noted. This may occur if the hyperons are made to pass through material before they decay. In our description of the proposed experimental set-up the decays occur in vacuum, so this is not a problem. However, alternative conceptualizations of the experiment should not neglect this point. The effect propagates linearly into the desired quantity A. Finally, we assume that the small precession of the spin vectors for the Λ and $\overline{\Lambda}$ in the residual magnetic field $\vec{B}$ around the production point are calculable or negligible.

Intrinsic to the discussion below is the asymmetry in the Λ and $\overline{\Lambda}$ decay distributions, momentum distributions and interactions with matter. This is also true for the decay products. The antiproton and proton are obviously quite different in their passage through detector material, and so are the π^+ and π^-, although to a lesser extent. The momentum and angular distributions of these decay particles are also different. While the region-of-interest defined in Section 8.2 reduces this effect when integrated over the accepted values of $\cos\theta^* \equiv \cos\theta^*_{\overline{\Lambda}}$, it still exists on the event-by-event basis where the

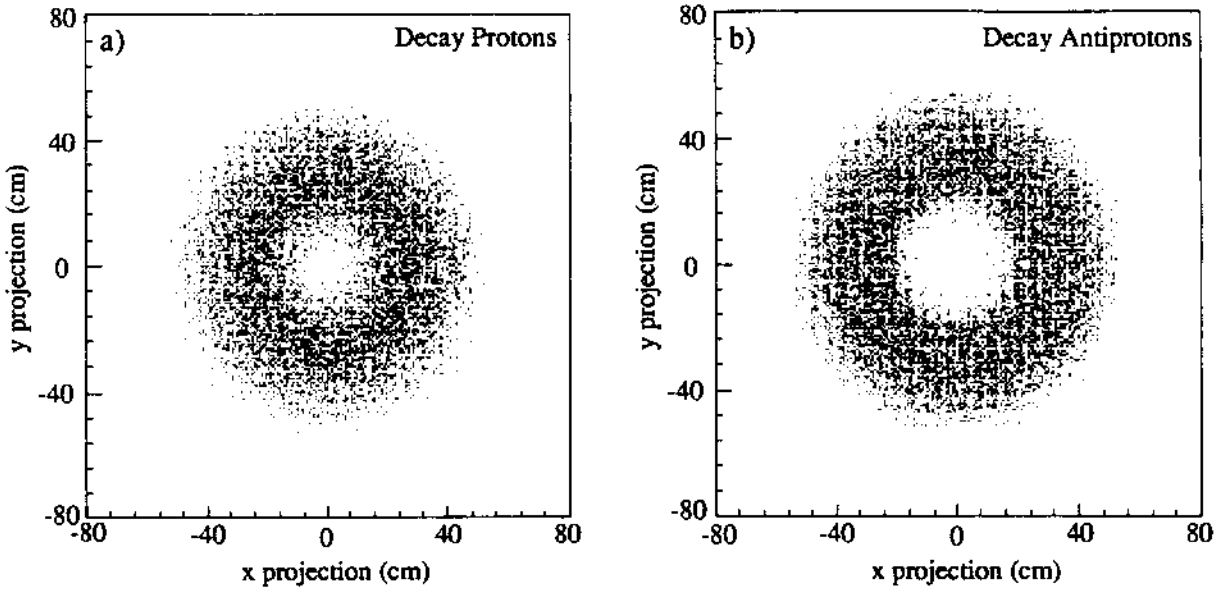

Figure 11: Radial impact of nucleons from $\overline{\Lambda}\Lambda \rightarrow \overline{p}\pi^+ p\pi^-$ decays. Events $\overline{p}p \rightarrow \overline{\Lambda}\Lambda \rightarrow \overline{p}\pi^+ p\pi^-$ at 1.65 GeV/c incident momentum were simulated according to the differential cross-section and differential polarization profile measured with PS185. Shown are the radial impacts of decay protons (a) and antiprotons (b). See text.

comparisons are made. For example, for a given non-zero value of $\cos\theta^*$, the Λ and $\overline{\Lambda}$ have different momenta. Accordingly they have different decay distributions downstream of the interaction point. Further, the decay products retain this difference. Since the region-of-interest spans $-0.75 \leq \cos\theta^* \leq +0.3$ (see Figure 3), more events where the Λ carries the greater fraction of the longitudinal momentum are included in the used distribution (see Figure 4). This means that the decay protons on average are located closer to the beam axis compared to the decay antiprotons. The antiproton-tagging calorimeter in the suggested detector design incorporates this selection window. This is easily seen by the radial impact of the region-of-interest events on a hypothetical spherical detector as shown in Figure 11 for the decay protons (a) and antiprotons (b). The distributions are different, but represent generated events according to the PS185 differential cross-section and differential polarization profile. The only cuts made are the exclusion of pions travelling with less than 40 MeV/c and the selection of the region-of-interest as defined above. The point is simply that the particles are being measured by different parts of the apparatus, hence they are *selectively sensitive* to efficiencies that may be a part of this apparatus.

Unfortunately, one cannot avoid this by choosing the region-of-interest to be symmetric in $\cos\theta^*$. While this would indeed make the decay distributions and momenta in the integrated sample overlap, the events which carry the statistical power into the determination of the quantity A remember the shape of the polarization distribution, and this is not symmetric about $\cos\theta^* = 0$ as shown in Figure 3.

10.2 Detector inefficiencies

Each event $\bar{p}p \to \overline{\Lambda}\Lambda \to \bar{p}\pi^+ p\pi^-$ is characterized by unique angles θ^* and ϕ^*, where θ^* is the $\overline{\Lambda}$ production angle in the $\bar{p}p$ centre-of-mass system and ϕ^* is the tilt of the $\overline{\Lambda}\Lambda$ production plane with respect to the horizontal. The number N^{++} refers to events, where the $\overline{\Lambda}$ is at angles θ^* and ϕ^*, the Λ is at angles $(\pi - \theta^*)$ and $(\phi^* + \pi)$, and both decay nucleons go upwards with respect to the production plane. The meaning of N^{--} is similar, but with both decay nucleons seen to go downwards.

Clearly, the most stringent requirement for the acceptance function η would be that for all angles θ^* and ϕ^*

$$\eta^{++}(\theta^*, \phi^*) = \eta^{--}(\theta^*, \phi^*) .$$

This means that at any given centre-of-mass production angle of the $\overline{\Lambda}$ and any given orientation of the production plane with respect the natural geometry of the detector, the acceptance for two nucleons going up or down is the same. One can easily imagine a simple scenario in which this is violated. Consider the tracking elements of an arbitrary detector being badly misaligned as in Figure 12 (a). The circle may represent, for example, the boundaries of the antiproton calorimeter and forward TOF hodoscope and thus defines the regions into which the nucleons must pass. We can simultaneously permit the pions to be measured with uniform efficiency without loss of generality. The beam travels along the positive z axis. Here we see by inspection the violation of equal efficiency for measuring up–up versus down–down events for particular values of ϕ^*. Uncorrected efficiency in this illustration is meant to be related to the visible area of active detector up or down with respect to the production plane.

A somewhat looser condition can be constructed to avoid this, namely the efficiency should have the symmetry

$$\eta^{++}(\theta^*, \phi^*) + \eta^{++}(\theta^*, \phi^* + \pi) = \eta^{--}(\theta^*, \phi^*) + \eta^{--}(\theta^*, \phi^* + \pi) .$$

This condition can be strictly satisfied only when both decays occur at the point of the original interaction as if the lifetime of the Λ and $\overline{\Lambda}$ was very short. Then events observed at a production plane of ϕ^* plus events observed at $(\phi^* + \pi)$ ought to have equal up–up and down–down efficiencies. But for the Λ and $\overline{\Lambda}$, the finite decay length removes this symmetry. The decay vertices occur at measurable distances with respect to the beam axis. Strictly speaking, this means that a reflection of any given event by π does not flip the detector seen by the given hyperon. A rotation is made, but a translation is also made. So, a simple efficiency hole in a quadrant will break this symmetry for particular values of θ^* and ϕ^*. This is illustrated in Figure 12 (b).

Finally, the weakest condition is the integral symmetry

$$\int_0^{2\pi} \eta^{++}(\theta^*, \phi^*) d\phi^* = \int_0^{2\pi} \eta^{--}(\theta^*, \phi^*) d\phi^* .$$

This means that the net efficiency difference for up–up versus down–down will vanish when all events are summed. Deviations enter due to second-order effects which will be demonstrated next.

With several simplifying assumptions we can illustrate how efficiency corrections tend to enter in second order in the azimuthal non-uniformity [46]. This has important implications on the level to which systematics must be controlled for a 10^{-4} measurement. We make the following assumptions.

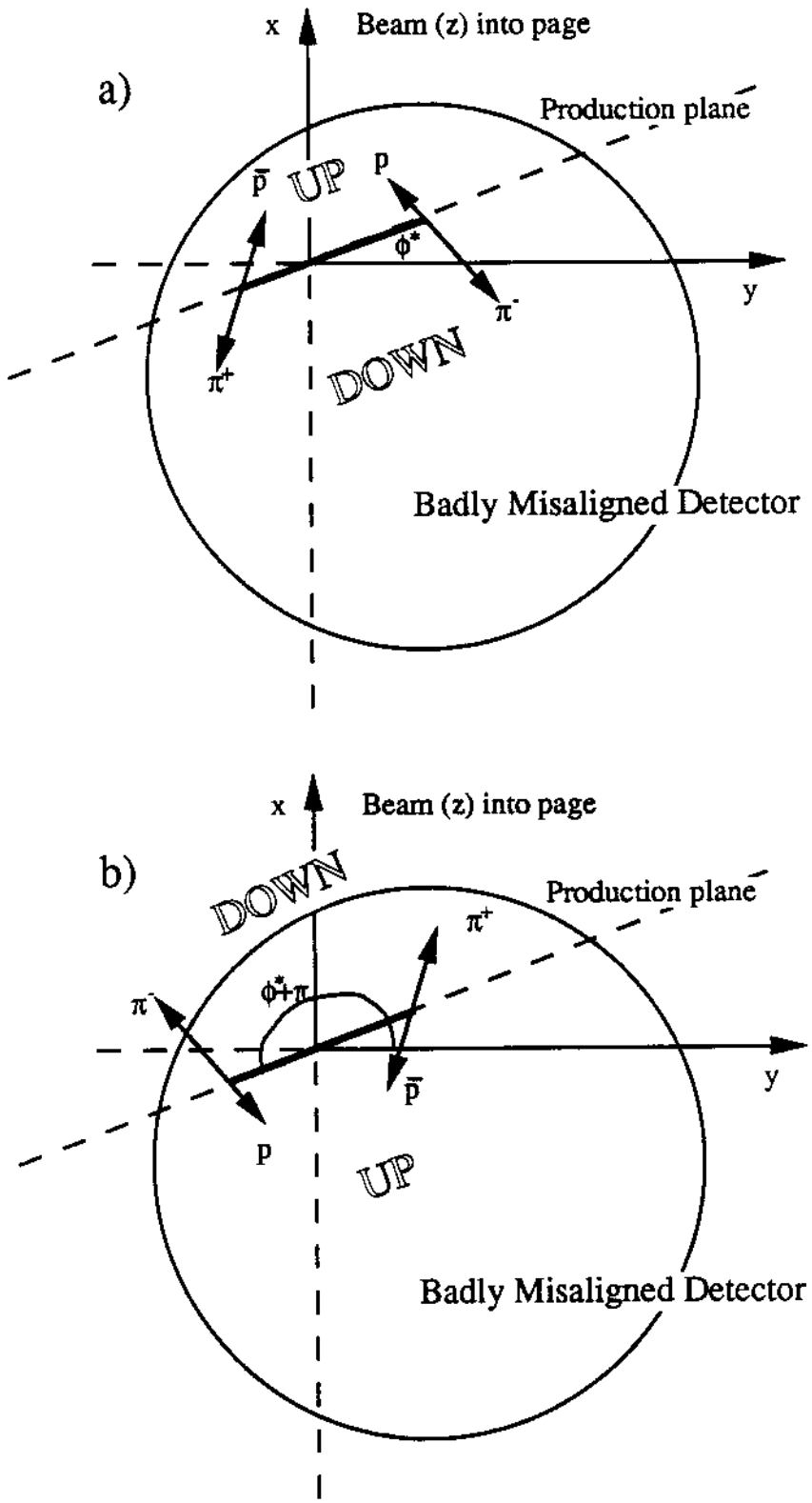

Figure 12: Systematic effects due to detector misalignment. Ilustrated are examples that would lead to the violation of equal efficiencies for measuring up–up versus down–down events for cases of a detector badly misaligned with respect to the beam axis. See text.

1. Assume that the π^+ and π^- are detected with 100 % efficiency, and that all systematic problems therefore come from the detection inefficiencies for decay protons and antiprotons.

2. Assume that the incident antiprotons and the target protons are unpolarized. Then the production process $\overline{p}p \rightarrow \overline{\Lambda}\Lambda$ is azimuthally symmetric. This is required in any case in order for $P_\Lambda(\pi - \theta^*) = P_{\overline{\Lambda}}(\theta^*)$, where $\theta^* \equiv \theta^*_{\overline{\Lambda}}$ is the centre-of-mass production angle of the $\overline{\Lambda}$ and P is the hyperon polarization.

3. Neglect the difference in the average decay lengths between the Λ and the $\overline{\Lambda}$, and assume therefore that the average spatial distributions of the decay vertices are the same.

4. Make use of the fact that the laboratory angle of the emitted proton is approximately along the direction of the decaying Λ, hence the detection efficiency for the Λ decay products can be written as $\eta(\psi, \phi)$, and assume the same correlation between the $\overline{\Lambda}$ and $\overline{p}$ directions. Here ϕ is the azimuthal angle of the p in the laboratory frame, and ψ is the polar production angle of the Λ in the laboratory frame. This is a fairly good approximation. Aside from the opposite signs of the decay asymmetries of the Λ and $\overline{\Lambda}$, the angular distribution of the proton and antiproton relative to the parent-particle spins is the same if they have the same production angles. Note that it would not be a good approximation to assume that the pions retain a memory of the hyperon direction, and this makes the extension of this discussion to include pion inefficiencies more complicated. The spirit of the calculation, however, remains. In a similar way, we define $\overline{\eta}(\overline{\psi}, \overline{\phi})$ for the efficiency in detecting $\overline{\Lambda}$ decay products. We can expand the efficiencies according to

$$\eta(\psi, \phi) = \sum_{n=0}^{\infty} \left[A_n(\psi) \cos n\phi + B_n(\psi) \sin n\phi \right] ,$$

$$\overline{\eta}(\overline{\psi}, \overline{\phi}) = \sum_{n=0}^{\infty} \left[\overline{A}_n(\overline{\psi}) \cos n\overline{\phi} + \overline{B}_n(\overline{\psi}) \sin n\overline{\phi} \right] .$$

5. Assume that the detection efficiencies for the Λ and the $\overline{\Lambda}$ decay products are uncorrelated. For example, we ignore possible tracking problems which arise when tracks are too close together to be distinguished from each other in the detector. The efficiency for detecting a good event is then

$$\eta_1(\psi, \overline{\psi}, \phi, \overline{\phi}) = \eta(\psi, \phi)\, \overline{\eta}(\overline{\psi}, \overline{\phi}) .$$

Using the fact that the incident antiproton beam and the target are unpolarized as discussed above, we can average the acceptance azimuthally over the detector:

$$\frac{1}{2\pi} \int_0^{2\pi} \eta_1(\psi, \overline{\psi}, \phi + \beta, \overline{\phi} + \beta)\, d\beta = A_0(\psi)\, \overline{A}_0(\overline{\psi}) +$$
$$\frac{1}{2} \sum_{n=1}^{\infty} \left[\left(A_n(\psi)\, \overline{A}_n(\overline{\psi}) + B_n(\psi)\, \overline{B}_n(\overline{\psi}) \right) \cos n(\overline{\phi} - \phi) + \right.$$
$$\left. \left(A_n(\psi)\, \overline{B}_n(\overline{\psi}) - B_n(\psi)\, \overline{A}_n(\overline{\psi}) \right) \sin n(\overline{\phi} - \phi) \right] .$$

The actual number of decay particles is proportional to

$$N(\psi, \cos\theta_p, \cos\theta_{\overline{p}}) = \sigma(\psi)\,[1 + P(\psi)(\alpha\cos\theta_p + \overline{\alpha}\cos\theta_{\overline{p}}) + \alpha\overline{\alpha}\,C_{yy}(\psi)\cos\theta_p\cos\theta_{\overline{p}}]\,,$$

where $\sigma(\psi)$ is the production cross-section, $P(\psi) = P_\Lambda(\pi - \theta^*) = P_{\overline{\Lambda}}(\theta^*)$ is the hyperon polarization, and θ_p is the angle of the decay proton in the Λ rest frame relative to the Λ polarization direction. In the spin-correlation term only the diagonal coefficient C_{yy} has been included for reasons of simplicity. With $u = (cos\theta_p + \cos\theta_{\overline{p}})/2$ and $v = (cos\theta_p - \cos\theta_{\overline{p}})/2$, we can rewrite this in the form

$$N(\psi, u, v) = \sigma(\psi)\,[1 + P(\psi)\,(\alpha + \overline{\alpha})\,u + P(\psi)\,(\alpha - \overline{\alpha})\,v + \alpha\overline{\alpha}\,C_{yy}(\psi)\,(u^2 - v^2)]\,.$$

The CP-violating signature is given by

$$2\alpha A \approx \alpha + \overline{\alpha} = \frac{N(\psi, u, v) - N(\psi, -u, v)}{2\,u\,P(\psi)}\,.$$

For our discussion, we will assume CP invariance, that is $\alpha + \overline{\alpha} = 0$, and see to what extent detector inefficiencies can cause a false CP-violation signal. Under this assumption, the above expression for N becomes

$$N(\psi, u, v) = \sigma(\psi)\,[1 + 2\,\alpha P(\psi)\,v + \alpha^2\,C_{yy}(\psi)\,(u^2 - v^2)]\,.$$

The actual number of detected particles is given by

$$n = \eta_1(\psi, \overline{\psi}, \phi, \overline{\phi})\,N(\psi, u, v)\,,$$

so that n must be corrected by the corresponding efficiency η_1 in order to calculate A. If η_1 is not sufficiently well-known, then a false CP signature and a non-zero value for $(\alpha + \overline{\alpha})$ can be induced.

In a more complete calculation, we can treat a given event at angles (ψ, ϕ) and $(\overline{\psi}, \overline{\phi})$ along with the companion events where $\Lambda \leftrightarrow \overline{\Lambda}$. Also, we can switch $\cos\theta_p \leftrightarrow -\cos\theta_{\overline{p}}$ for these two events, which means $u \leftrightarrow -u$ and leaves v invariant. Thus there are four related events to be considered. Then we find [46]

$$\alpha + \overline{\alpha} = \frac{\sum_{n=1}^{\infty}\,[\sin n(\overline{\phi} - \phi)\,Z_n]}{2\,u\,\langle P\rangle\,[N(\overline{\psi}, -u, v)A_0(\psi)\,\overline{A}_0(\overline{\psi}) + N(\psi, u, v)\,A_0(\overline{\psi})\,\overline{A}_0(\psi)]}\,,$$

where we have defined

$$Z_n = N(\overline{\psi}, -u, v)\,[A_n(\psi)\,\overline{B}_n(\overline{\psi}) - B_n(\psi)\,\overline{A}_n(\overline{\psi})] + N(\psi, u, v)\,[A_n(\overline{\psi})\,\overline{B}_n(\psi) - B_n(\overline{\psi})\,\overline{A}_n(\psi)],$$

$$\langle P\rangle = \frac{N(\psi, u, v)\,P(\psi) + N(\overline{\psi}, -u, v)\,P(\overline{\psi})}{N(\psi, u, v) + N(\overline{\psi}, -u, v)}\,,$$

and we have neglected higher-order terms in the denominator. Clearly, a non-zero value of $(\alpha + \overline{\alpha})$ is a false CP-violation signature.

We note that all factors are of the type $A_n\overline{B}_n$ or $B_n\overline{A}_n$. The even component of one distribution in ψ couples with the odd component of the other distribution in $\overline{\psi}$. Therefore, the largest effects would be produced by asymmetries in detector efficiencies when the events are orthogonal in azimuth. The terms A_0, B_0, $\overline{A}_0$, and $\overline{B}_0$ are azimuthally

symmetric, hence they do not appear in the expression for $(\alpha+\overline{\alpha})$. Consequently, there is no false CP-violation signal generated when the detector is azimuthally symmetric, under the approximations listed above.

The non-uniform terms, A_n and B_n with $n \geq 1$, contribute quadratically to $(\alpha+\overline{\alpha})$. Consequently, if these terms could be held to 0.01 or smaller, then the generated error is at the desired level of 10^{-4} or less. Non-uniformities at the level of 0.01 can be measured relatively easily using the $\overline{\Lambda}\Lambda$ data itself or for example data from the reaction $\overline{p}p \rightarrow \overline{p}p\pi^+\pi^-$.

We can examine a couple of special cases. If $N(\psi,u,v) = N(\overline{\psi},-u,v)$, which is not true in general, we could still fake CP violation if $A_n(\psi) \neq \overline{A}_n(\psi)$ or if $B_n(\psi) \neq \overline{B}_n(\psi)$, that is if the detection efficiencies for p and $\overline{p}$ were not the same. In the actual case, where $N(\psi,u,v) \neq N(\overline{\psi},-u,v)$, CP violation can be faked even if $A_n(\psi) = \overline{A}_n(\psi)$ or if $B_n(\psi) = \overline{B}_n(\psi)$, since the numerator in the above expression takes on the form

$$[N(\psi,u,v) - N(\overline{\psi},-u,v)]\,[A_n(\psi)\,B_n(\overline{\psi}) - A_n(\overline{\psi})\,B_n(\psi)]\,.$$

While the quadratic nature of the non-uniformities is encouraging, a more detailed study, including pions and with fewer approximations, is required.

10.3 Some cures

Various sensible tests can be employed to probe the degree of uniformity of the acceptance function. One can analyze all events to evaluate the Λ and $\overline{\Lambda}$ lifetimes. This means that the difference in lifetimes has the full statistical power of the number of analyzed events, irrespective of the polarization factor which dilutes the symmetry for CP. A measurement of the lifetime difference using 2×10^9 events would give a high-precision test of CPT. Of course, one would interpret the lifetime measurement *not* as a CPT test but rather as a test of the uniformity of the detector acceptance.

Another test is to take in parallel the complementary reaction $\overline{p}p \rightarrow \overline{p}p\pi^+\pi^-$ which naturally satisfies the on-line trigger. This reaction has a cross-section about three times lower than the $\overline{p}p \rightarrow \overline{\Lambda}\Lambda$ production cross-section at 1.65 GeV/c. However, like for the lifetime measurement, all events can be used. Here one would use these events to determine the efficiency of the detector. The final-state particles are distributed in an azimuthally symmetric way, again provided that the beam and target are unpolarized.

Finally, we propose to use the event sample itself in the following manner to test for systematic effects. To begin, we recall that the observation of the polarization distribution (see Figure 3) is made by measuring the up–down asymmetry for a given hyperon decay *with respect to the* $\overline{\Lambda}\Lambda$ *production plane*. On an event-by-event basis, this plane can be chosen (in the off-line analysis) to be oriented, instead, in an arbitrary direction with respect to the vertex location. The choice for this *wrong-plane analysis* could be along some natural physical orientation of the detector such as the horizontal or vertical divisions. This wrong plane is then used to determine the up–down asymmetry for the hyperon decay. By definition, a null result must be produced for the polarization of both hyperon and antihyperon. Further, the actual CP-counting statistics of up–up versus down–down events can be calculated in this same manner. For a bias-free detector, we must then get $N^{++} = N^{--}$ and $N^{+-} = N^{-+}$.

10.4 Simple illustrations

To illustrate the type of effects that could generate a false CP signal, we have made a number of Monte Carlo simulations. A representative calculation of four case studies is presented here. It should be noted that these are preliminary studies. The results are summarized in Table 1. The relevant quantity $(\alpha + \overline{\alpha})$ is calculated from the difference up–up to down–down type events, where the sense of up or down is taken using the *true production plane*. Additionally, as a test of the uniformity of the detector, we have evaluated the event totals representing the four types N^{++}, N^{--}, N^{+-}, N^{-+}, when a *wrong plane* such as the horizontal (X) or vertical (Y) division of the detector is chosen for analyzing the sense of up or down on each event. We include in the table the ratios N^{++}/N^{--} and N^{+-}/N^{-+} as well as the errors on these ratios. For a symmetric detector the wrong-plane ratios should equal unity. The general features of the cases are as follows.

- *Case I.* Fully efficient detector, $\alpha = -\overline{\alpha}$. We expect and we see no CP violation for any of the true-plane or wrong-plane choices. The detector is symmetric in the wrong-plane analyses as expected.

- *Case II.* Fully efficient detector, $\alpha = -0.9\,\overline{\alpha}$. We see CP violation at the required level in the true-plane analysis, but none in the wrong-plane analyses. Again, the detector is symmetric. The observed CP violation is real.

- *Case III.* The detector has a peculiar efficiency property like that illustrated in Figure 13 (a). It is blind to protons in the hatched azimuthal wedge, while being blind to antiprotons in the solid azimuthal wedge, the sectors being orthogonal in azimuth and 18° wide here. Otherwise, all particles are measured with equal efficiency. Here, the input is $\alpha = -\overline{\alpha}$. A small CP violation is seen in the true-plane analysis. Much larger anomalies occur in the wrong-plane analyses, which indicate efficiency problems with respect to the X- and Y-planes.

- *Case IV.* The detector has an efficiency problem like that illustrated in Figure 13 (b). It is blind to *both* protons and antiprotons in the hatched and solid regions. These regions, however, are respectively nearer to and further from the beam axis. Thus, they represent different regions of sensitivity to protons and antiprotons for the region-of-interest events. Again, the input is $\alpha = -\overline{\alpha}$, but here we see false CP violation in the true-plane analysis. This is a type of second-order systematic error which must be considered. Fortunately, the wrong-plane analyses also show a clear difficulty.

To summarize, the systematic problems in the proposed experiment must be considered in much greater detail. Speaking in general terms, one finds that the measurement of A can be biased and a CP-violating asymmetry be faked through effects of higher order. By this we mean combinations of two or more effects, for instance those that may arise from misalignment of detectors, non-uniformity of detectors, nucleon–pion misidentification, and wrong assignment of Λ and $\overline{\Lambda}$ vertices. Since the decay products are necessarily different, it is easy to introduce these second-order effects for the efficiencies alone. However, any detector inefficiency having *full azimuthal symmetry* cannot fake CP violation, because it still fulfills the condition of a *CP-invariant detector*. Faking CP violation means a selective loss of events, either of the up–up or of the down–down type. This is possible

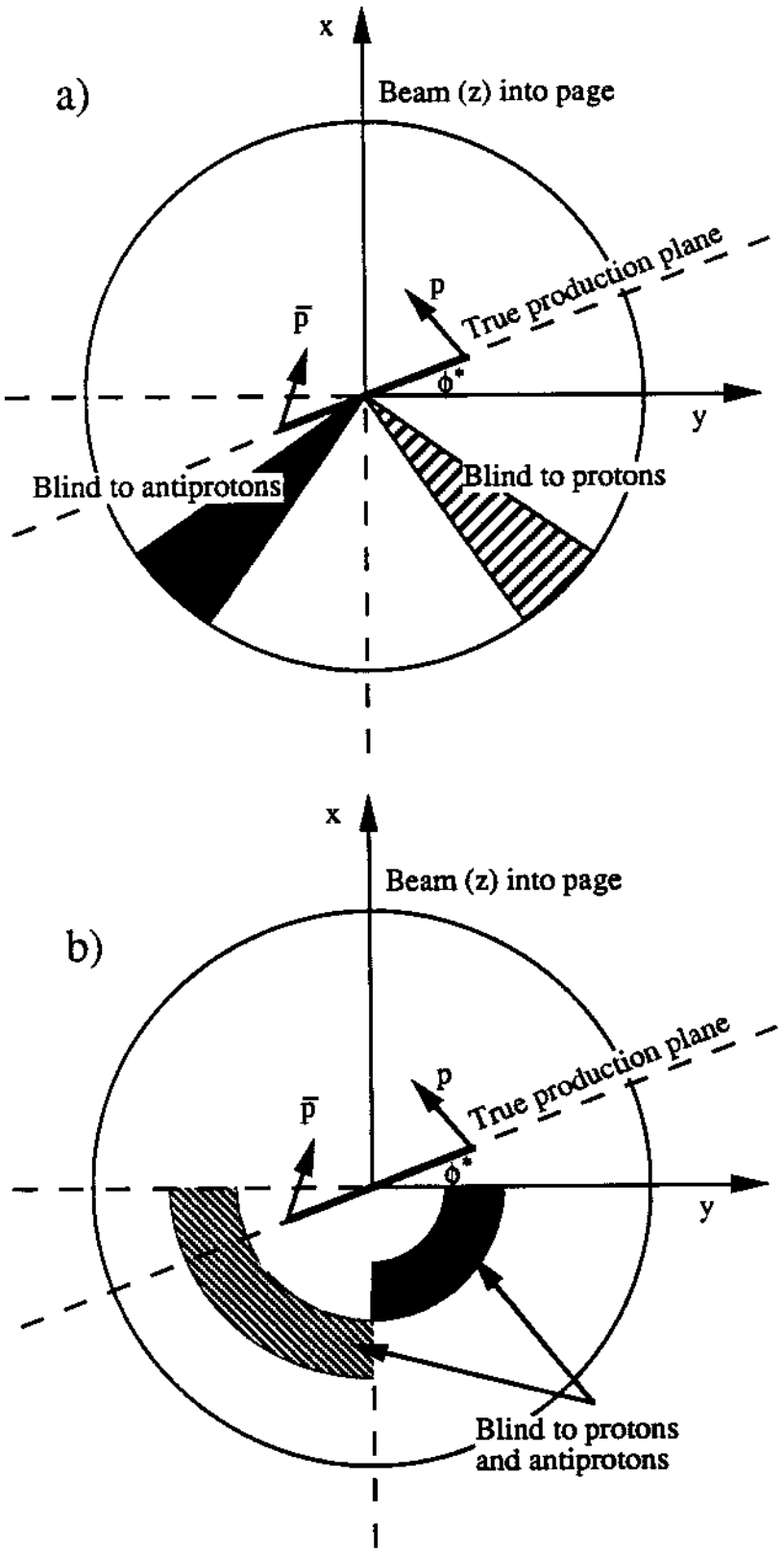

Figure 13: Some peculiar cases of detection inefficiencies. Illustrated are examples of selective detection inefficiencies which are non-symmetric in azimuth and may contribute to false CP violation. See text, where the cases III and IV correspond to (a) and (b), respectively.

Case	Anal. plane	$\alpha+\overline{\alpha}$	N^{++}/N^{--}	N^{+-}/N^{-+}
I. $\alpha=-\overline{\alpha}$	Prod. plane	0.0048 ± 0.0047	0.9980 ± 0.0028	1.6980 ± 0.0049
Full efficiency	X-plane		0.999 ± 0.007	1.0010 ± 0.0021
	Y-plane		1.007 ± 0.007	0.9971 ± 0.0021
II. $\alpha=-0.9\,\overline{\alpha}$	Prod. plane	0.0677 ± 0.0047	0.9724 ± 0.0028	1.6539 ± 0.0048
Full efficiency	X-plane		0.997 ± 0.007	1.0011 ± 0.0021
	Y-plane		1.006 ± 0.007	1.0031 ± 0.0021
III. $\alpha=-\overline{\alpha}$	Prod. plane	0.0093 ± 0.0051	0.9961 ± 0.0016	1.716 ± 0.0015
Holes, Fig. 13 (a)	X-plane		1.614 ± 0.004	1.041 ± 0.001
	Y-Plane		0.679 ± 0.004	0.820 ± 0.001
IV. $\alpha=-\overline{\alpha}$	Prod. plane	0.111 ± 0.006	0.9552 ± 0.0034	1.678 ± 0.006
Holes, Fig. 13 (b)	X-plane		1.279 ± 0.011	2.735 ± 0.008
	Y-Plane		0.660 ± 0.005	0.9879 ± 0.0026

Table 1: Results from case studies of detector inefficiencies. The four cases listed are described in the text. For the true-plane analysis, a deviation of $(\alpha+\overline{\alpha})$ from the input value, or, for the wrong-plane analysis, a deviation of the event-number ratios N^{++}/N^{--} or N^{+-}/N^{-+} from unity, indicate false CP violation.

only by means of inefficiencies that are azimuthally localized and selectively act on Λ or $\overline{\Lambda}$ decay products.

Finally, we believe that the efficiencies and other systematic sources can be controlled in order to achieve the desired result at the 10^{-4} level. Clearly, a very careful understanding of the detector, the choice of detector materials, and the reconstruction procedures will be required in order to obtain a large sample of unbiased events. Since the experiment will span more than a year of running, additional tests may have to be envisioned which satisfy the early-to-late run correspondences.

11 Conclusions

One of the fundamental questions in particle physics is that of the physical origin of CP non-invariance. If $|\Delta S| = 1$ direct CP violation exists it may be observable in the non-leptonic decays of hyperon–antihyperon pairs, $\overline{\Lambda}\Lambda \to \overline{p}\pi^+ p\pi^-$ or $\overline{\Xi}^-\Xi^- \to \overline{\Lambda}\pi^+\Lambda\pi^- \to \overline{p}\pi^+\pi^+ p\pi^-\pi^-$. Given the constraints provided within the context of the Standard Model, differences in the decay-asymmetry parameters are presently estimated for $\overline{\Lambda}\Lambda \to \overline{p}\pi^+ p\pi^-$ to be of the order of a few times 10^{-5} to 10^{-4}. This is clearly beyond the scope of previous experiments. However, the high-quality data on $\overline{\Lambda}\Lambda$ cross-sections and polarizations measured with PS185 at LEAR provide important information about the feasibility of a new experiment with which to reach a higher level of accuracy for the CP-violation observables. Based on existing data as well as studies on statistics and systematic effects, the conclusion is that a measurement of $A = (\alpha+\overline{\alpha})/(\alpha-\overline{\alpha})$ with a precision $\sigma_A \approx 10^{-4}$ is feasible by analyzing a large sample of $N \approx 2\times 10^9$ events $\overline{p}p \to \overline{\Lambda}\Lambda \to \overline{p}\pi^+ p\pi^-$. These can be produced at the LEAR-2 machine, which has to be optimized for and temporarily dedicated to such an experiment. After exploratory measurements of cross-sections and polarizations in $\overline{p}p \to \overline{\Xi}^-\Xi^-$ at SuperLEAR, a high-statistics study of the double self-analyzing decays in $\overline{p}p \to \overline{\Xi}^-\Xi^- \to \overline{\Lambda}\Lambda \to \overline{p}\pi^+ p\pi^-$ can be envisaged as well. If a non-zero

signal of CP violation in a hyperon–antihyperon decay channel is measured, it would constitute first evidence that the violation of CP invariance is not an isolated phenomenon of the $K^0 - \overline{K}^0$ system but a universal feature in weak interactions of strange particles.

Acknowledgements

We are indebted to Pierre Darriulat for his stimulating interest in and his significant contributions to the work presented here. We also acknowledge enjoyable discussions with Pierre Lefèvre and Dieter Möhl on LEAR-2 machine aspects.

A Reaction $\overline{p}p \to \overline{\Xi}^-\Xi^- \to \overline{\Lambda}\pi^+\Lambda\pi^-$ at SuperLEAR

A.1 Distribution of decay angles and polarizations

In principle, the cleanest measure of CP violation in hyperon decays is given by the ratio $B' = (\beta+\overline{\beta})/(\alpha-\overline{\alpha})$, for which both the decay asymmetry and the final-state polarization have to be detected [21, 28]. The unique process with which to do this is $\overline{p}p \to \overline{\Xi}^-\Xi^-$, the neutral channel $\overline{\Xi}^0\Xi^0$ being more difficult for experimental reasons. Due to the required beam momenta around 3.5 GeV/c the reaction is not accessible at LEAR. However, at SuperLEAR it will open up an exciting field of double $s\overline{s}$ quark dynamics and spin physics. After an exploratory phase, a search for CP violation can be envisaged as a second stage of the experiment [22, 23, 24].

In $\overline{p}p \to \overline{\Xi}^-\Xi^-$ the reaction products exhibit a sequence of two self-analyzing delayed decays, which together allow B' and B to be determined. The first decay, $\overline{\Xi}^-\Xi^- \to \overline{\Lambda}\pi^+\Lambda\pi^-$ (with $c\tau = 4.91$ cm), measures the parameters α of Ξ^- and $\overline{\alpha}$ of $\overline{\Xi}^-$ by means of the up–down asymmetry of the decay angular distributions ($\alpha = -0.456 \pm 0.014$ for the Ξ^-). In the second decay, $\overline{\Lambda}\Lambda \to \overline{p}\pi^+p\pi^-$ (with $c\tau = 7.89$ cm), the parameters β of Ξ^- and $\overline{\beta}$ of $\overline{\Xi}^-$ are determined by measuring the Λ and $\overline{\Lambda}$ polarizations from the up–down asymmetry of their decay angular distributions ($\alpha = 0.642 \pm 0.013$ for the Λ).

It is assumed that the hyperons produced in $\overline{p}p \to \overline{\Xi}^-\Xi^-$ emerge with a polarization transverse to the production plane, $\vec{S}_{\Xi^-} = P_{\Xi^-}\,\hat{y}$. In the Ξ^- rest frame the decay Λ particles exhibit an angular distribution of the form

$$I(\theta_\Lambda) = \frac{1}{4\pi}\,(1 + \alpha\vec{S}_{\Xi^-}\cdot\hat{p}_\Lambda) = \frac{1}{4\pi}\,[1 + (\alpha P)_{\Xi^-}\cos\theta_\Lambda]\,,$$

where $\theta_\Lambda \equiv \theta_{\Lambda_y}$ is measured between the normal to the production plane and the Λ direction in the Ξ^- rest frame, hence $\cos\theta_\Lambda = \hat{y}\cdot\hat{p}_\Lambda$. The decay Λ particles are longitudinally polarized in the Ξ^- rest frame, the Λ polarization being dependent on the initial Ξ^- polarization and on the Λ emission angle [48]. The Λ polarization in the Ξ^- rest frame is calculated as [21, 49]

$$\vec{S}_\Lambda = \frac{(\alpha + \vec{S}_{\Xi^-}\cdot\hat{p}_\Lambda)\hat{p}_\Lambda + \beta(\vec{S}_{\Xi^-}\times\hat{p}_\Lambda) + \gamma\,[\hat{p}_\Lambda\times(\vec{S}_{\Xi^-}\times\hat{p}_\Lambda)]}{1 + \alpha\vec{S}_{\Xi^-}\cdot\hat{p}_\Lambda}\,.$$

The decay angular distribution $I(\theta_\Lambda)$ and the final-state hyperon polarization $\vec{S}_\Lambda$ can both be derived in a straightforward way from the decay matrix element.

The above formula shows how the polarization of the decay Λ in the Ξ^- rest frame is described in terms of three orthogonal components given by the unit vectors $\hat{e}_3 = \hat{p}_\Lambda$, $\hat{e}_2 = \hat{S}_{\Xi^-} \times \hat{p}_\Lambda$, and $\hat{e}_1 = \hat{p}_\Lambda \times (\hat{S}_{\Xi^-} \times \hat{p}_\Lambda)$. These Λ polarization components have the following explicit form [49]:

$$P_{\Lambda_3} = \frac{\alpha + P_{\Xi^-} \cos\theta_\Lambda}{1 + (\alpha P)_{\Xi^-} \cos\theta_\Lambda} ,$$

$$P_{\Lambda_2} = \frac{\beta P_{\Xi^-} \sin\theta_\Lambda}{1 + (\alpha P)_{\Xi^-} \cos\theta_\Lambda} ,$$

$$P_{\Lambda_1} = \frac{\gamma P_{\Xi^-} \sin\theta_\Lambda}{1 + (\alpha P)_{\Xi^-} \cos\theta_\Lambda} .$$

Using this coordinate system, Lorentz-transformed along $\hat{p}_\Lambda$ from the Ξ^- into the Λ rest frame, the angular distribution of the decay protons is then given by three equations:

$$I(\theta_{p_i}) = \frac{1}{4\pi}(1 + \alpha \vec{S}_{\Lambda_i} \cdot \hat{p}_p) = \frac{1}{4\pi}[1 + (\alpha P)_{\Lambda_i} \cos\theta_{p_i}] ,$$

where $\cos\theta_{p_i} = \hat{e}_i \cdot \hat{p}_p$ and $i = 1, 2, 3$. In the actual experiment the angular distributions of two consecutive decays are measured, $\Xi^- \to \Lambda\pi^-$ and $\Lambda \to p\pi^-$. These are described by the four equations for $I(\theta_\Lambda)$ and $I(\theta_{p_i})$. The polarization as well as the decay parameters α and β of the Ξ^- hyperons can be extracted simultaneously from the data [48]. The $\overline{\Xi}^-$ observables are determined correspondingly.

A CP-violating asymmetry involving the decay parameters β and $\overline{\beta}$ is [21]

$$\check{B} = \vec{S}_{\Xi^-} \cdot (\vec{S}_\Lambda \times \vec{p}_\Lambda - \vec{S}_{\overline{\Lambda}} \times \vec{p}_{\overline{\Lambda}}) .$$

The Ξ^- polarization is in the direction normal to the production plane, $\hat{y}$, and the Λ polarization is manifest by the direction of the decay-proton momentum, $\vec{p}_p$. The above triple-product correlation can then be transformed into the asymmetry

$$\check{B} = \hat{y} \cdot (\vec{p}_p \times \vec{p}_\Lambda - \vec{p}_{\overline{p}} \times \vec{p}_{\overline{\Lambda}}) .$$

Integrating over the total number N of events, the up–down counting asymmetry becomes [21]

$$\tilde{B} = \frac{[N_p(up) - N_{\overline{p}}(up)] - [N_p(down) - N_{\overline{p}}(down)]}{N} \propto P_{\Xi^-}\, \alpha_\Lambda\, (\beta + \overline{\beta})_{\Xi^-} ,$$

where up (down) refers to $\hat{y} \cdot [\vec{p}_p \times \vec{p}_\Lambda] > 0\ (< 0)$ in the Ξ^- rest frame. Using the same notation as in the $\overline{\Lambda}\Lambda$ case for the numbers of decay protons (first superscript) and antiprotons (second superscript) going up (+) or down (−) with respect to the $\overline{\Xi}^-\Xi^-$ production plane, we obtain

$$\tilde{B} = 2\,\frac{N^{+-} - N^{-+}}{N} ,$$

where $N = N^{++} + N^{+-} + N^{-+} + N^{--}$ is the total number of events.

A.2 Experimental considerations

Data on the reaction $\overline{p}p \rightarrow \overline{\Xi}^{-}\Xi^{-}$ are very scarce [50]. The cross-section estimates come from a few bubble-chamber experiments, and they are based on a handful of identified events or, in some cases, on the non-observation of such events. The reaction threshold is at $\sqrt{s} = 2.643$ GeV, which corresponds to 2.621 GeV/c incident antiproton momentum in a fixed-target experiment. From some existing data around 3.5 GeV/c we conclude that the $\overline{p}p \rightarrow \overline{\Xi}^{-}\Xi^{-}$ production cross-section is $\sigma \approx 2\ \mu b$ at this energy. The branching ratio for (2+4) charged particles in the final state is 41 %. We note, that the cross-section of the reaction $\overline{p}p \rightarrow \overline{\Lambda}\Lambda\pi^{+}\pi^{-}$ is an order of magnitude larger, and substantial contributions to this are due to the $\Sigma(1385)$ resonances. However, the distinct kinematical features of $\overline{p}p \rightarrow \overline{\Xi}^{-}\Xi^{-}$ and the subsequent chain of delayed decays should make it possible to identify these events uniquely in the off-line analysis and to separate them from the background.

Nothing is known experimentally about the angular distribution and the hyperon polarization in the exclusive process $\overline{p}p \rightarrow \overline{\Xi}^{-}\Xi^{-}$. Although it is appealing to assume that there are similarities with $\overline{p}p \rightarrow \overline{\Lambda}\Lambda$, the double quark–antiquark annihilation and creation process embedded in $\overline{p}p \rightarrow \overline{\Xi}^{-}\Xi^{-}$ may imply quite a different dynamical behaviour. The inclusive production of hyperons in proton–proton and proton–nucleus interactions indicates [51] that the Ξ^{-} particles emerge with a polarization somewhat smaller than that of the Λ. Clearly, the pursuit of a search for CP violation with $\overline{p}p \rightarrow \overline{\Xi}^{-}\Xi^{-}$ must be preceded, as a first and in itself interesting step, by detailed measurements of cross-sections and spin variables of that reaction.

Monte Carlo events, $\overline{p}p \rightarrow \overline{\Xi}^{-}\Xi^{-}$ at 3.5 GeV/c incident antiproton momentum, were generated isotropically in the centre-of-mass system [22]. The simulations showed that all baryons are confined within a laboratory cone of $\theta^{lab} \leq 40°$, and almost all pions go into the forward hemisphere. This indicates what an experiment on $\overline{p}p \rightarrow \overline{\Xi}^{-}\Xi^{-}$ should look like. The detector should have the characteristics of a wide-angle forward decay spectrometer with a fiducial volume sufficiently large in longitudinal and transverse directions. A pilot experiment for measurements of cross-sections and spin variables of $\overline{p}p \rightarrow \overline{\Xi}^{-}\Xi^{-}$ would be best pursued using an extracted beam at SuperLEAR, hence it should be in spirit somewhat similar to the $\overline{p}p \rightarrow \overline{\Lambda}\Lambda$ experiments performed with PS185 at LEAR.

A high-statistics measurement of $\overline{p}p \rightarrow \overline{\Xi}^{-}\Xi^{-}$ calls for highest luminosities, therefore it implies the use of an internal target. A peak luminosity $L_0 = 10^{32}\ cm^{-2}s^{-1}$ is foreseen for SuperLEAR when operated with a hydrogen-cluster jet target [44]. Near 3.5 GeV/c beam momentum the production rate of events $\overline{p}p \rightarrow \overline{\Xi}^{-}\Xi^{-} \rightarrow \overline{\Lambda}\pi^{+}\Lambda\pi^{-} \rightarrow \overline{p}\pi^{+}\pi^{+}p\pi^{-}\pi^{-}$ is estimated to be $n_0 \approx 80\ s^{-1}$ at peak luminosity, not accounting for non-perfect experimental acceptances. When considering the relevant production cross-sections, and the relative sizes of the CP-testing ratios, it appears conceivable that an experiment on $\overline{p}p \rightarrow \overline{\Xi}^{-}\Xi^{-}$ aiming at $\sigma_{B'} \approx 10^{-3}$ requires a running time similar to that of a $\overline{p}p \rightarrow \overline{\Lambda}\Lambda$ experiment with $\sigma_A \approx 10^{-4}$. An experiment designed for $\overline{p}p \rightarrow \overline{\Xi}^{-}\Xi^{-}$ measurements would naturally be suited for $\overline{p}p \rightarrow \overline{\Lambda}\Lambda$ studies as well. The change between the two processes merely involves modifications of the on-line trigger conditions.

B Hadronic J/ψ decays at a τ–charm factory

The DM2 experiment [52] at the Orsay–DCI e^+e^- storage ring investigated radiative and hadronic J/ψ decays. From a total of 8.6×10^6 recorded $e^+e^- \rightarrow J/\psi$ events, 1847 hadronic decays $J/\psi \rightarrow \overline{\Lambda}\Lambda \rightarrow \overline{p}\pi^+ p\pi^-$ were isolated. The quantity evaluated was the scalar product of the unit vectors of the decay proton and antiproton momenta in the Λ and $\overline{\Lambda}$ rest frames, $\hat{p}_p \cdot \hat{p}_{\overline{p}}$. The distribution extracted from the data was compared to the one obtained from a Monte Carlo simulation performed under the assumption of CP invariance. The difference between the experimental data and the simulation was quantified by adopting the known α value and varying $\overline{\alpha}$. As a result of this minimization procedure the product $\alpha\overline{\alpha}$ was obtained, from which $A = 0.01 \pm 0.10$ was deduced [52].

The method of using $J/\psi \rightarrow \overline{\Lambda}\Lambda$ decays does not explicitly require the equality of Λ and $\overline{\Lambda}$ polarizations. It seems appealing also in view of the well-defined quantum numbers $J^{PC} = 1^{--}$ of the J/ψ and $\overline{\Lambda}\Lambda$ systems. On the other hand, the method does require an extremely good understanding of the measured momentum distributions of the outgoing protons and antiprotons, hence it relies heavily on Monte Carlo simulations. A major statistical problem is the small $J/\psi \rightarrow \overline{\Lambda}\Lambda$ branching ratio, which is determined [4] to be $(1.35 \pm 0.14) \times 10^{-3}$. One can estimate that the precision $\sigma_A \approx 10^{-4}$ corresponds to $N \geq 1.8 \times 10^9$ analyzed events, just like in the $\overline{p}p$ case.

Future e^+e^- colliders [53] operating in the energy region of a few GeV, called *τ–charm factories* (τcF), aim at a peak luminosity as large as $L_0 = 10^{33}\ cm^{-2}s^{-1}$ for the optimal collision energy E_0. Assuming $L \propto E^2$, one has $L = 6 \times 10^{32}\ cm^{-2}s^{-1}$ when running on the J/ψ resonance. Owing to the small width of the J/ψ, the visible production cross-section $\sigma(e^+e^- \rightarrow J/\psi)$ depends strongly on the spread of the collision energy σ_E. For the values $\sigma_E = 1$ MeV and 0.1 MeV the relevant cross-sections are 2.8 μb and 18.9 μb, respectively. With the known branching ratios for $J/\psi \rightarrow \overline{\Lambda}\Lambda \rightarrow \overline{p}\pi^+ p\pi^-$ it follows that the production rate of useful events is 0.9 s^{-1} to 6.3 s^{-1} at peak luminosity, not accounting for non-perfect experimental acceptances [54]. Even under the more optimistic assumptions for σ_E, which imply the use of beam monochromators, such event rates are lower at least by a factor 250 when compared to a realistic $\overline{p}p \rightarrow \overline{\Lambda}\Lambda \rightarrow \overline{p}\pi^+ p\pi^-$ scenario as that described in this report. Therefore, one is clearly led to the conclusion that the τ–charm factory is *not competitive* for the accumulation of a large-statistics sample of $\overline{\Lambda}\Lambda$ decays.

However, it should be pointed out that the τ–charm factory may be an interesting alternative to $\overline{p}p$ for the $\overline{\Xi}^-\Xi^-$ case [31, 54], in contrast to the $\overline{\Lambda}\Lambda$ case. The relevant branching ratio [4], $BR(J/\psi \rightarrow \overline{\Xi}^-\Xi^-) = (1.8 \pm 0.4) \times 10^{-3}$, is similar to $BR(J/\psi \rightarrow \overline{\Lambda}\Lambda)$, but the measurement of B or B' in $\overline{\Xi}^-\Xi^-$ decays requires much less events than that of A in $\overline{\Lambda}\Lambda$ decays [31].

References

[1] PS185 Collaboration, Memorandum CERN/PSCC/83–6 (1983).

[2] Minutes of the 64th Meeting of the Proton Synchrotron and Synchro-cyclotron Experiments Committee, CERN/PSCC/90–27 (1990).
Minutes of the 99th Meeting of the Research Board, CERN/DG/RB 90–159 (1990).
Report on the Cogne V Meeting of the PSCC, CERN/PSCC/90–32 (1990).

[3] J.H. Christenson et al., Phys. Rev. Lett. 13 (1964) 138.

[4] Particle Data Group, Phys. Lett. 239B (1990) 1.
For a comparison see also the previous edition: Phys. Lett. 204B (1988) 1.

[5] H. Burkhardt et al., Phys. Lett. 206B (1988) 169.

[6] G. Barr, "Proc. Joint International Lepton–Photon Symposium and Europhysics Conference on High-Energy Physics", Geneva, 1991, to be published.

[7] J.R. Patterson et al., Phys. Rev. Lett. 64 (1990) 1491.

[8] B. Winstein, "Proc. Joint International Lepton–Photon Symposium and Europhysics Conference on High-Energy Physics", Geneva, 1991, to be published.

[9] For reviews see: L.–L. Chau, Phys. Rep. 95 (1983) 1;
L. Wolfenstein, Annu. Rev. Nucl. Part. Sci. 36 (1986) 137.

[10] M. Kobayashi and K. Maskawa, Prog. Theor. Phys. 49 (1973) 652.

[11] C. Jarlskog, in: "CP Violation", ed. C. Jarlskog (World Scientific, Singapore, 1989), p. 3.

[12] For a review see: F. Dydak, "Proc. 25th International Conference on High-Energy Physics", Singapore, 1990, eds. K.K. Phua and Y. Yamaguchi (World Scientific, Singapore, 1991), p. 3.

[13] For a survey see: J.F. Donoghue, B.R. Holstein and G. Valencia, Int. Journ. Mod. Phys. A2 (1987) 319.

[14] G.D. Barr et al., Proposal CERN/SPSC/90–22 (1990), approved as experiment NA48.

[15] L. Adiels et al., Proposal CERN/PSCC/85–6 (1985), approved as experiment PS195.
R. Adler et al., preprint CERN–PPE/92–32 (1992).

[16] See for example: G. Barbiellini et al., Particle World 1 (1990) 138;
D.B. Cline, preprint UCLA–CAA–0079 (1991);
A. Calcaterra, preprint LNF–91/070 (1991).

[17] A. Pais, Phys. Rev. Lett. 3 (1959) 242.

[18] O.E. Overseth and S. Pakvasa, Phys. Rev. 184 (1969) 1663.

[19] T. Brown, S.F. Tuan and S. Pakvasa, Phys. Rev. Lett. 51 (1983) 1823.

[20] L.–L. Chau and H.–Y. Cheng, Phys. Lett. 131B (1983) 202.

[21] J.F. Donoghue and S. Pakvasa, Phys. Rev. Lett. 55 (1985) 162.
J.F. Donoghue, B.R. Holstein and G. Valencia, Phys. Lett. 178B (1986) 319.

[22] N.H. Hamann, preprint CERN–EP/89–69 (1989), and "Proc. Workshop on CP Violation at KAON Factory", TRIUMF, Vancouver, 1988, ed. J.N. Ng, report TRI–89–3 (1989), p. 29.

[23] D.W. Hertzog, "Proc. Symposium/Workshop on Spin and Symmetries", TRIUMF, Vancouver, 1989, eds. W.E. Ramsay and W.T.H. van Oers, report TRI–89–5 (1989), p. 89.

[24] G. Bassompierre, preprint CERN–EP/89–106 (1991).

[25] G. Buchalla, A.J. Buras and M.K. Harlander, Nucl. Phys. B337 (1990) 313.

[26] E.A. Paschos and Y.L. Wu, Mod. Phys. Lett. A6 (1991) 93.

[27] L. Wolfenstein, Phys. Rev. Lett. 13 (1964) 562.

[28] J.F. Donoghue, X.–G. He and S. Pakvasa, Phys. Rev. D34 (1986) 833.

[29] J.F. Donoghue, "Proc. 3rd Conference on the Intersections between Particle and Nuclear Physics", Rockport, 1988, ed. G.M. Bunce, (AIP Conference Proceedings No. 176, American Institute of Physics, New York, 1988) p. 341.

[30] M.J. Iqbal and G.A. Miller, Phys. Rev. D41 (1990) 2817.

[31] X.–G. He, H. Steger and G. Valencia, Phys. Lett. 272B (1991) 411.

[32] F.S. Crawford et al., Phys. Rev. 108 (1957) 1102.
F. Eisler et al., Phys. Rev. 108 (1957) 1353.

[33] T.D. Lee and C.N. Yang, Phys. Rev. 108 (1957) 1645.

[34] L. Durand, III, and J. Sandweiss, Phys. Rev. 135 (1964) B540.

[35] R. Gatto, Phys. Rev. 108 (1957) 1103.

[36] P. Chauvat et al., Phys. Lett. 163B (1985) 273.

[37] P.D. Barnes et al., Nucl. Phys. A526 (1991) 575.

[38] P.D. Barnes et al., Phys. Lett. 199B (1987) 147.

[39] H. Fischer, Dissertation, University of Freiburg, in preparation.

[40] M.L. Faccini–Turluer, Z. Phys. C1 (1979) 19.

[41] D. Besset et al., Nucl. Instr. and Meth. 166 (1979) 515.

[42] N.H. Hamann, "Proc. SuperLEAR Workshop", Zürich, 1991, to be published.

[43] P. Lefèvre, talk presented at the "Cogne V Meeting of the PSCC", Cogne, 1990, CERN/PSCC/90–28 (1990).

[44] G. Cesari et al., "Proc. SuperLEAR Workshop", Zürich, 1991, to be published.

[45] W. Kubischta, private communication.

[46] P. Darriulat, internal notes (1991).
See also: G. Zech, talk presented at the "Cogne V Meeting of the PSCC", Cogne, 1990, CERN/PSCC/90–28 (1990).

[47] L. Wolfenstein, Phys. Rev. D43 (1991) 151.

[48] J. Bensinger et al., Nucl. Phys. B252 (1985) 561.
D. Aston et al., Phys. Rev. D32 (1985) 2270.

[49] W. Koch, in: "Analysis of scattering and decay", ed. M. Nikolić (Gordon and Breach, New York-London-Paris, 1968), p. 231.

[50] High-Energy Reactions Analysis Group, report CERN–HERA/84–01 (1984).

[51] For a review see: L.G. Pondrom, Phys. Rep. 122 (1985) 57.
For an update see: J. Lach, preprint FERMILAB–Conf–91/200 (1991).

[52] M.H. Tixier et al., Phys. Lett. 212B (1988) 523.

[53] See for example: J. Kirkby, Particle World 1 (1989) 27;
M.L. Perl and R.H. Schindler, preprint SLAC–PUB–5666 (1991);
N. Wermes, preprint HD–PY 91/4 (1991).

[54] E. Gonzaléz, preprint CIEMAT 676 (1991).